JOURNAL OF OCEAN AND CLIMATE

Original Article

Journal of Ocean and Climate
Volume 9: 1–24

DOI: 10.1177/2516019219866569
journals.sagepub.com/home/ocs
SAGE

WAM and WAVEWATCH-III intercomparison studies in the North Indian Ocean using Oceansat-2 Scatterometer winds

J Swain[1], PA Umesh[1,2] and AN Balchand[3]

Abstract

This paper presents the intercomparison of wave hindcasts using the third-generation models WAM and WAVEWATCH-III for the North Indian Ocean over 1° × 1° (latitude × longitude) grid resolutions, which reveals the first assessment of their relative performance through intercomparison of the model results. Hindcast wave parameters such as significant wave height, mean wave period, and swell wave height obtained from the simulations using Oceansat-2 scatterometer winds are analyzed to understand the quality and variability associated with the individual model outputs in the Indian Ocean. WAM and WAVEWATCH-III intercomparison studies are carried out for four different cases (January and June 2010, and January and June 2011). A comparative study of the relative performances of these two models is evaluated through extensive and robust statistical error analysis. Based on both qualitative and quantitative assessment of the model results, this study clearly indicates that both WAM and WAVEWATCH-III performed well in the common model domain using Oceansat-2 scatterometer winds, and they can be confidently used for long-term hindcasting in the North Indian Ocean, which will be very useful for most of the user community dealing with various coastal/offshore activities. The study also suggests that it would be preferable to consider available long-term wave measurements both in deep and coastal waters of the North Indian Ocean to validate and intercompare WAM and WAVEWATCH-III further.

Keywords

WAM, WAVEWATCH-III, wave hindcast, wave model intercomparison, Oceansat-2 scatterometer winds

Date received: 10 March 2018; accepted: 8 June 2019

Introduction

The knowledge of the ocean environment and its temporal and spatial variabilities is essential for various defense and civilian applications. Therefore, the forecasting of ocean surface waves is a problem of great practical interest, as the sea-state impacts virtually all aspects of naval operations as well as a variety of commercial and maritime activities. Accurate wave information, including waves of extreme weather events, is very essential for a wide range of research and engineering applications. Wave statistics derived from point measurements were considered for obtaining reliable local wave climate in the past. However, these measurements are not sufficient to describe the regional wave patterns over a long period of time. This emphasizes the need to work on wave models driven by wind fields obtained from satellite measurements or weather prediction model wind forecasts. Today, the third-generation wave models are capable of predicting the waves reasonably well, and the accuracies can be still

[1]Naval Physical and Oceanographic Laboratory, Kochi, Kerala, India
[2]Department of Civil Engineering, Indian Institute of Technology Bombay, Mumbai, India
[3]Department of Physical Oceanography, Cochin University of Science and Technology, Kochi, Kerala, India

Corresponding author:
PA Umesh, Department of Civil Engineering, Indian Institute of Technology Bombay, Mumbai 400 076, India.
Emails: umeshpa.nair@gmail.com; umeshpa@iitb.ac.in

improved with appropriate representation of extremely complex physical processes of wind-generated waves (Polnikov et al., 2007; Vledder, 2001). Researchers have developed a series of third-generation models such as WAM (WAM; WAMDI Group, 1988), WAVEWATCH-III (WWIII; Tolman, 2009; Tolman et al., 2002), and Simulating Waves Nearshore (SWAN; Booij et al., 1999; Ris et al., 1999; SWAMP Group, 1985), which are widely being applied for global as well as regional sea-state forecasts. The components of source function are used without prior restrictions on the spectral shape. The shallow water wave model SWAN (Ris et al., 1999) has been designed specifically for coastal wave prediction, and it is utilized in several coastal regions around the world.

The state-of-the-art third-generation wave models and their prospects by Holthuijsen (2007), Komen et al. (1994), and the WISE Group (2007) can be referred for more details. It may be noted that, like many other geophysical phenomena, waves can also be studied on very different space and temporal timescales (Lavrenov, 2003). Oceanic storms belong to large-scale phenomena and are mainly related to the processes of wind momentum transfer, nonlinear transfer, current refraction, and turbulent dissipation of energy. As waves move toward the shore, other physical processes become important, namely, refraction induced by sudden variations in depth (or by coastal currents) and shoaling. Since the forcing now become increasingly dependent on regional currents and local variations in bathymetry, the scale of the problem becomes smaller. In most situations, the two types of waves can still be analyzed within the framework of the same theory. As a result, a third-generation wave model like WAM, which efficiently solves the kinetic equation and the source functions in order to give global and regional forecasts, can be combined with other models like SWAN that are more oriented toward propagation on the coastal scale. We further refer to Janssen (2008) and Komen et al. (1994) for a complete description of WAM, and to Booij et al. (1999) and the SWAN Team (2011) for information on SWAN. The global WWIII model, operational at the National Centers for Environmental Prediction (NCEP), was first developed for shelf sea applications by Tolman (1991), and is gaining wide acceptance in the wave forecasting community. It is similar to WAM in structure, but incorporates wave–current interactions, a more sophisticated third-order numerical propagation scheme, new formulations of wind input, and dissipation source terms (Tolman and Chalikov, 1996). The WWIII model solves the spectral action density balance equation in the wavenumber-directional domain. Like WAM, WWIII assumes that the wave spectrum and medium variations (water depth and surface current field) vary on time and space scales much larger than those for a single wave, and thus can only be applied on spatial scales larger than a few kilometers and outside the surf zone, because the physics is not valid for regions of severely depth-limited waves. Considering the recent advances in the availability of computer power, it has become feasible to use a chain of numerical models to connect the wave propagation from a larger model domain to the smaller regional/coastal scales. The resulting system can provide not only large-scale wave forecasts based on synoptic-scale wind and satellite data assimilation, but also a realistic ongoing description of the coastal processes in smaller regional areas.

Wave model intercomparison studies have been reported across the globe by various researchers till date (Hanson et al., 2009; Korres et al., 2011; Ortiz-Royero and Mercado-Irizarry, 2008; Padilla-Hernandez et al., 2007; Tolman et al., 2002). With the increasing demand for modernization, there is an equally increasing demand to forecast ocean waves (Rusu, 2011) in open sea and coastal areas to aid marine applications. Many users and the scientific community depend on nowcasts and ocean state forecasts for marine-related operations (Balakrishnan Nair et al., [2013] 2014; Sandhya et al., 2014). WAM studies for the North Indian ocean using WAM, WWIII, and SWAN have been carried out by several researchers such as Amrutha et al. (2016), Nayak et al. (2013), and Sabique et al. (2012). Few researchers have used coupled modeling system (Warner et al., 2010; Zeng et al., 2015) consisting of several state-of-the-art modeling components, including the Regional Ocean Modeling System (ROMS) for ocean and sediment transport, and the SWAN model for ocean waves. Hanson et al. (2009) evaluated the performance of three numerical wave models (WAM Cycle 4.5, WWIII, and WAVAD) in the Pacific basin. The three models exhibited varied performance in the depiction of wind-sea and young swells in their physical attributes. WWIII hindcasts exhibited consistently higher performance scores than those from WAM and WAVAD. The prediction of mature swells in the winter months, with elevated height errors in all three models, was a noteworthy problem. In another study, three state-of-the-art operational forecast wave models, WAM, WWIII, and SWAN, were compared through simulations (Padilla-Hernandez et al., 2007) of two severe winter storms in the northwest (NW) Atlantic. Model performances were also evaluated through comparisons/validations with field measurements. The results revealed that, although the models are comparable in terms of their overall performance and skill, it was found that WWIII provides (Padilla-Hernandez et al., 2007) a better statistical fit to the observed wave data compared with the other models, and that SWAN gives slightly better results if nested within WWIII, rather than within WAM. Tolman et al. (2002) reported that for Japan, the Gulf of Mexico, and the NW Atlantic, NWWIII (National Oceanic and Atmospheric Administration (NOAA) WWIII) appears to be significantly better than WAM, primarily based on the regression slopes. For the Northeast (NE) Pacific and Atlantic, NWWIII has much better correlation coefficients and smaller standard deviations

and root-mean-square errors (RMSE) than WAM. However, NWWIII overestimates the slope of the regression line by 16%, whereas WAM underestimates the slope by a much smaller percentage.

A systematic intercomparison of WAM Cycle 4 and WWIII wave model results has been reported for the Mediterranean region by Korres et al. (2011). The intercomparison of the two wave models over the whole Mediterranean basin showed that noticeable differences in terms of significant wave height (Hs) and periods (Hs RMS differences of 0.5–0.7 m and wave period RMS differences of 1.5–2.0 s) was seen along the track of the main cyclones over the basin, where the swell contribution to the wave field was important. In the geographic areas of the Mediterranean Sea where wind-seas dominate, the two models exhibit almost the same performance. Intercomparison of SWAN and WWIII with buoy observations was carried out by Ortiz-Royero and Mercado-Irizarry (2008). The study tested the applicability of the SWAN model at oceanic scales. Although comparison between buoy observations and model outputs tends to favor WWIII over SWAN in deep waters, it was stressed that the ease of using SWAN, together with the simplification offered by just having to learn to use one model, makes the SWAN model a good option for simulations all the way from deep waters up to the nearshore.

In an operational scenario, to verify the efficiency of model computed parameters, systematic validation studies with long-term observational data are an essential prerequisite to improve the prediction capability and enhancement of wave model performances. A long-term intercomparison of model computed wave parameters for the North Indian Ocean region is, however, missing. The novelty of this work is the intercomparison of two modeling systems, namely, WAM and WWIII, to suggest the suitability and capabilities for their future utilization and exploitation in predicting the sea-state information required for various practical applications. In this study, significant wave parameters such as Hs and mean wave period (Tm) are validated first using buoy measurements and, hence, leading to intercomparison of model output parameters such as Hs, Tm, and swell wave height (Hsw). The intercomparison study gives reasonably good results with low RMSE and high correlation coefficients. This study is going to be the first, but initial attempt to intercompare each of the models such as WAM C4.5.3 and WWIII V3.14 for the North Indian Ocean region, purposely to find acceptance and project its usefulness on sea-state information such that hindcast results will be acceptable with more confidence.

Wave models

WAM Cycle 4.5.3 and WAVEWATCH-III V3.14

The WAM model solves a spectral equation for describing the evolution of the two-dimensional (2D) wave spectrum. WAM Cycle 4.5 is an update of the WAM Cycle 4 wave model, which is described in Gunther et al. (1992) and Komen et al. (1994). The basic physics and numerics are kept in the new release. The source function integration scheme developed by Bidlot et al. (2005) and Hersbach and Janssen (1999) and is used in WAM Cycle 4.5.3. A number of additional options are added in the new model release WAM Cycle 4.5.3 (Gunther and Behrens, 2011). The new method is semi-implicit and is based on the latest developments at ECMWF (Janssen, personal communication). The wave model dissipation source function has been reformulated in terms of a mean steepness parameter and mean frequency that give more emphasis on the high-frequency part of the spectrum and result in a more realistic interaction between wind-sea and swell waves. This has allowed relaxation of the prognostic frequency range over which the model equations are integrated. A few other small adjustments were also necessary to take advantage of the increased dynamic range of the model (Bidlot et al., 2005). More details on WAM can be found in the works of Gunther and Behrens (2011), Gunther et al. (1992), and Komen et al. (1994).

WWIII (Version 3.14) is a WAM-type ocean surface wave model developed at NOAA/NCEP (Tolman, 2009; Tolman and Chalikov, 1996). It has been successfully used in global and regional scale studies in many areas including the North Atlantic, and has proven to be an effective tool to study wave spectral evolution, air–sea interactions, and nonlinear wave–wave interactions. WWIII is a discrete spectra and phase averaged model (Battjes, 1994). For regional and global applications, the directional wave spectrum is resolved at each model grid point in terms of wavenumber-direction bands and the evolution of the wave field is found by numerically solving the spectral wave action balance equation. More details on the WWIII model used in this study are available in the works by Tolman (2009).

Data and methodology

Oceansat-2 winds

Oceansat-2 is the second Indian satellite dedicated to ocean research, a continuity of the operational services of Oceansat-1 with high potential applications launched in September 2009. It has onboard Ku-band pencil beam scatterometer, the Oceansat-2 scatterometer (OSCAT), the Ocean Color Monitor (OCM) for oceanographic studies, and the radio occultation sounder for atmosphere (ROSA) for meteorological applications. The Indian Space Research Organisation (ISRO) reprocessed OSCAT Level-2B (L2B) global data (Version 1.3, released in December 2011) of wind speed and direction with a high spatial resolution of 50×50 km^2 (with targeted accuracies of 10% (RMS) and 20° (RMS) in the wind speed and wind direction) obtained from the Oceansat-2 data portal of

Table 1. Details of wave model implementations, validation, and intercomparisons using WAM and WWIII for the North Indian Ocean.

	WAM Cycle 4.5.3	WWIII (V3.14)
Model domain	Global (0°–360°E and 77°S to 77°N)	Global (0°–360°E and 77°S–77°N)
Grid spatial resolution	1° × 1°	1° × 1°
Spectral discretization	25 frequencies and 24 directions	25 frequencies and 24 directions
First frequency	0.04177	0.0412
Last frequency	0.41145	0.4056
Wave physics	Deep water	Deep water
Wind	Oceansat-2 (50 × 50 km^2)	Oceansat-2 (50 × 50 km^2)
Wind input	6-hourly (January and June 2010) 6-hourly (January and June 2011)	
Wave outputs	6-hourly (January and June 2010) 6-hourly (January and June 2011)	
Model output parameters for validation using NIOT buoys	Significant wave height and mean wave period	
Model output parameters for intercomparison	Significant wave height, mean wave period, and swell wave height	
Data used for validation (NIOT buoys)	January 2011: BD14 (off Sri Lanka) June 2011: BD08 (off Paradip), BD11 (off Nellore), and BD14	

National Remote Sensing Centre (NRSC; www.nrsc.gov.in) for selected months of the years 2010 and 2011. OSCAT has a repeat cycle of 2 days with the equatorial crossing time of 12 PM ± 10 minutes orbiting at an altitude of 720 km and inclination of 98.25° (Chakraborty and Raj Kumar, 2013; Jayaram et al., 2014; Sudha and Prasada Rao, 2013; Udaya Bhaskar et al., 2016). In this study, the OSCAT measured winds are subjected to spatiotemporal interpolation (Swain et al., 2017) and the 6-hourly gridded wind fields are generated over 1° × 1° resolution to drive the wave models WAM and WWIII. In the study by Swain et al. (2017), the accuracy of OSCAT winds has been reported. The comparison of interpolated OSCAT winds with buoy measurements such as RAMA, PIRATA, and TRITON over the Indian, Pacific, and Atlantic Oceans revealed reasonably good agreements with a correlation coefficient (R) greater than 0.8 and a mean deviation 1.04 m/s (for the wind speed range of 1–16 m/s) and 25° for wind speed and direction, respectively.

Model setup and methods

The third-generation wave models WAM (Cycle 4.5.3) and WWIII (Version 3.14) are implemented to intercompare with each other using OSCAT winds. WAM (Gunther and Behrens, 2011) and WWIII (Tolman, 2009) are implemented for the globe covering the geographical extents of 0°–360°E and 77°S to 77°N with a resolution 1° × 1°, in order to cater for the swells propagating from the Southern Ocean into the study domain (North Indian Ocean). Considering the global simulations, model outputs are extracted from both WAM and WWIII to carry out the validations and intercomparisons in the North Indian Ocean (0° N to 30°N; 50°E to 100°E; 1° × 1°), as described in Table 1. Figure 1 shows the study/model area, such as the North Indian Ocean, with buoy locations used for the validation (green solid circles) and selected locations for intercomparison (blue solid circles) between WAM and WWIII. Apart from the input OSCAT winds, the other model forcings such as current data used as input for wave models are obtained from the Ocean Surface Current Analyses Real-time (OSCAR) database (Bonjean and Lagerloef, 2002). The model bathymetry (Figure 1) has been constructed from ETOPO2 data. The ERA-interim daily fields from ECMWF were used for extracting the air–sea temperature difference data as input for WWIII. All models consider current refraction for the evolution of 2D wave spectra for the full degrees of freedom. WWIII additionally considers air–sea temperature difference. The WAM model uses 25 frequencies ranging from 0.04177 to 0.41145 Hz and 12 directions (constant increment) to represent the wave spectral evolution. Similarly, WWIII uses 25 frequencies ranging from 0.0412 to 0.4056 Hz, with a logarithmic distribution with increment factor 1.1 and 24 directions (constant increment). The wave model was executed for the whole global grid, whereas the model outputs have been extracted only for the regional domains (0°–30°N; 50°E–100°E) of interest. Source integration and propagation time steps were set to 10 and 20 minutes, respectively, for the global model executions. Table 1 shows the details of wave model implementation, validations, and intercomparisons using WAM and WWIII for the North Indian Ocean.

In this study, OSCAT winds for the months of January and June (2010 and 2011) have been used for driving the wave models. WAM and WWIII intercomparison studies have been carried out for four different cases (January and June 2010; January and June 2011) based on the

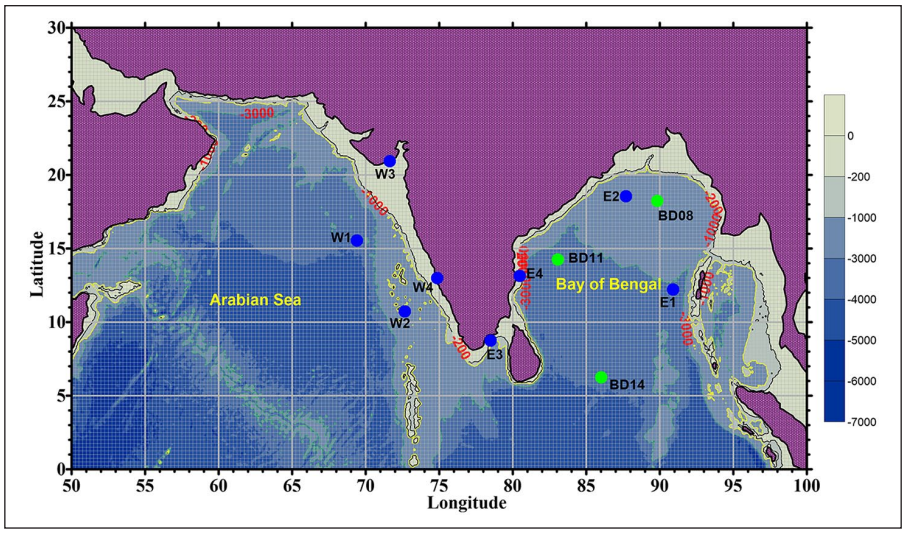

Figure 1. Map showing locations of wave rider buoys (green solid circles) for validation and selected locations (blue solid circles) in the North Indian Ocean utilized for WAM and WWIII intercomparisons.

availability of quality wave measurements for validating the associated model outputs before their intercomparisons. The significant wave parameters considered for this intercomparison study are Hs, Tm, and Hsw. Comparisons have been carried out for the North Indian Ocean for the above selected months using analyzed (OSCAT) winds as input fields. To evaluate the relative model performances based on the intercomparison studies for the case studies considered, an extensive statistical error analysis was carried out based on monthly wave hindcasts. The most suitable statistical measures such as correlation coefficient (R), scatter index (SI), bias (B, mean deviation), RMSE, percentage error (PE), and model performance index (MPI) between the model outputs (WAM and WWIII) have been computed and examined to evaluate their relative performances.

Bias (B) is a statistical quantity that signifies the average difference between model output and the in-situ measurement (Padilla-Hernandez et al., 2007). The bias value is good to reveal general trends in the model performance, that is, if the model consistently over- or underpredicts the measurements. RMSE is an absolute measure of fit between the model data and the buoy measurement. The lower value of RMSE indicates a better fit of data between model and observations. SI is expressed as a measure of the goodness of fit between the model and the measurements. The scatter index does not reveal general trends, but is good to evaluate the average model performance. The correlation coefficient (the R value) is used to measure the strength and direction of relationship between two variables (observed and predicted). The relationship can be either positive or negative depending on the directionality of the estimate (Remya et al., 2012). To better diagnose the model performance from a modeling point of view, PE and MPI are used (Brown, 2010; Ris et al., 1999). PE is defined as the difference between measured and hindcast parameters, as a percentage of the observed value. The diagnostic MPI indicates the degree to which the model reproduces the observed changes in the waves. However, it is essential to note here that the estimates, such as RMSE and PE, between the two models not involving sea-truth measurements are also relative assuming that one of the model is the benchmark, say WAM in this case. Therefore, the interpretations of RMSE, PE, and bias are treated accordingly during the discussion of results.

Results and discussion

Wave hindcasts using OSCAT winds

The 6-hourly interpolated OSCAT wind fields were utilized as inputs to force the WAM and WWIII for wave hindcasting during January and June 2010, and January and June 2011. Brief analysis based on both these cases is given below.

The spatial distribution of sample input wind fields for the North Indian Ocean (25th, 12:00 hours) is shown for the months of January and June 2010. Figure 2(a) and (b) shows the wind speed which varied from 2 to 6 m/s and 6 to 14 m/s, respectively, for 25 January 2010, 12:00 hours, and 25 June 2010, 12:00 hours. It may be seen from these plots that the wind speed and direction for January and June 2010 represent the standard climatic pattern of wind variability (Hastenrath and Lamb, 1979; Young and Holland, 1996), north-easterly for 25 January 2010, 12:00 hours and south-westerly for 25 June 2010, 12:00 hours.

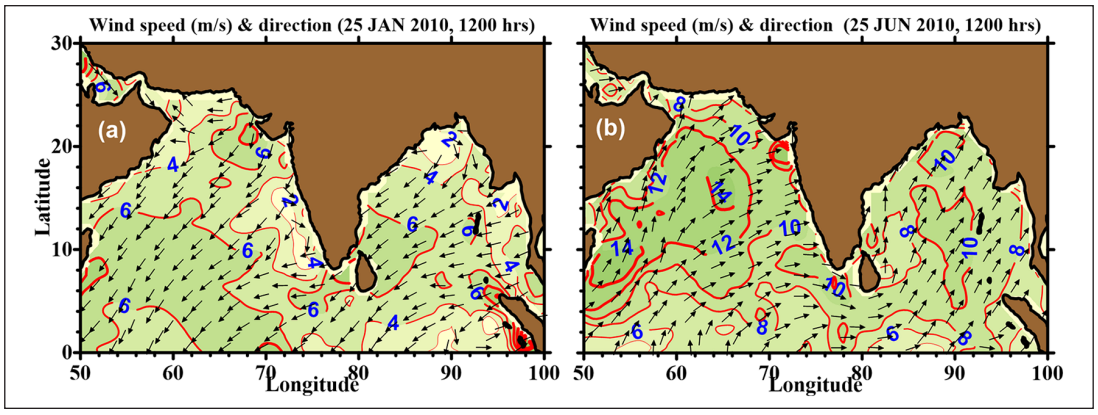

Figure 2. Input wind field (OSCAT), wind speed (m/s), and direction (arrows) for wave hindcast using WAM and WWIII for the North Indian Ocean, January and June 2010.

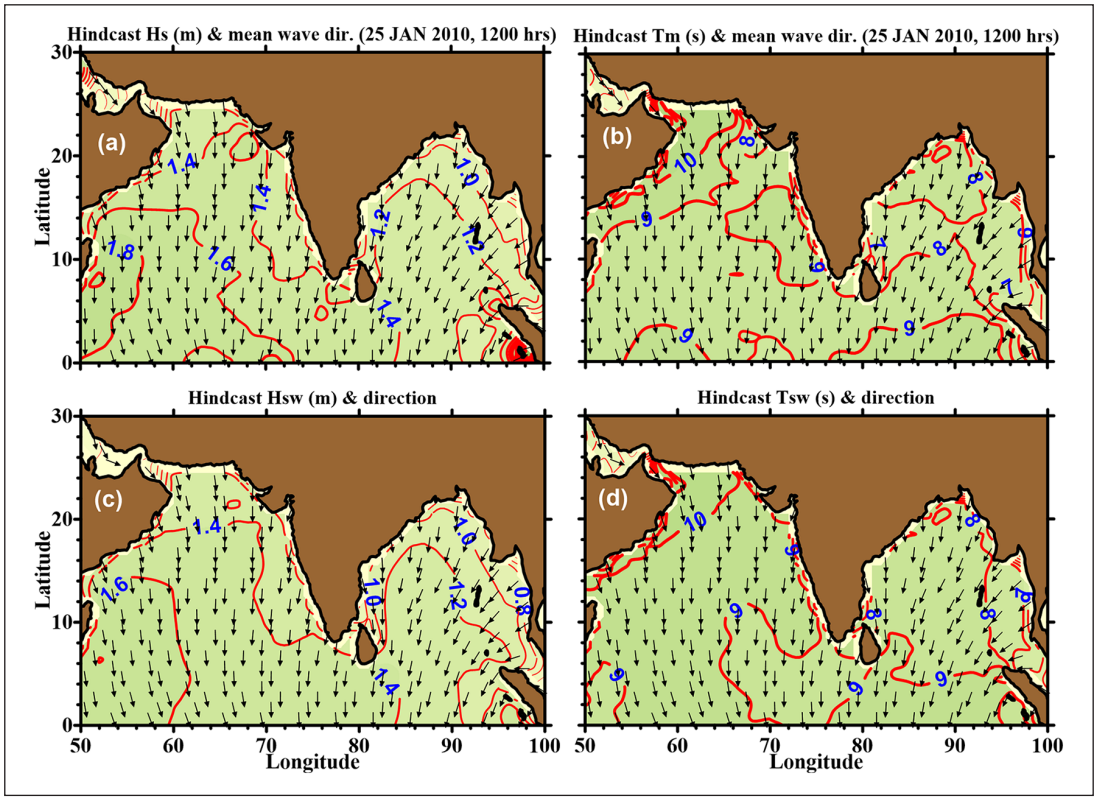

Figure 3. WAM hindcast wave fields (Hs, Tm, Hsw, and Tsw) using OSCAT winds, 25 January 2010, 12:00 hours.

The WAM hindcast wave fields such as Hs, Tm, Hsw, Tsw, and the wave directions for 25 January 2010, 12:00 hours are shown in Figure 3. Hs varied from about 1.4 to 1.8 m in the Arabian Sea and 1.0 to 1.4 m in the Bay of Bengal. Tm varied between 8 and 10 s in the Arabian Sea, whereas it varied from 7 to 9 s in the Bay of Bengal. The mean wave directions more or less agree with the wind pattern. Hsw ranged from 1.4 to 1.8 m in the Arabian Sea and from 0.8 to 1.4 m in the Bay of Bengal. Tsw varied from 8 to 10 s in the Arabian Sea and from 6 to 9 s in the Bay of Bengal. Figure 4 shows the WAM hindcast wave fields for 25 June 2010, 12:00 hours using OSCAT winds. Here, Hs ranged between 2.0 and 4.5 m in the Arabian Sea and between 1.0 and 2.5 m in the Bay of Bengal. Tm varied from 8 to 11 s in the Arabian Sea and from 6 to 10 s in the Bay of Bengal. In the Bay of Bengal, Hsw varied from 1.0 to 2.5 m, while in the Arabian Sea, it varied from 1.5 to 3.0 m. Tsw varied in the Arabian Sea between 12 and 13 s, and in Bay of Bengal, it varied between 8 and 11 s.

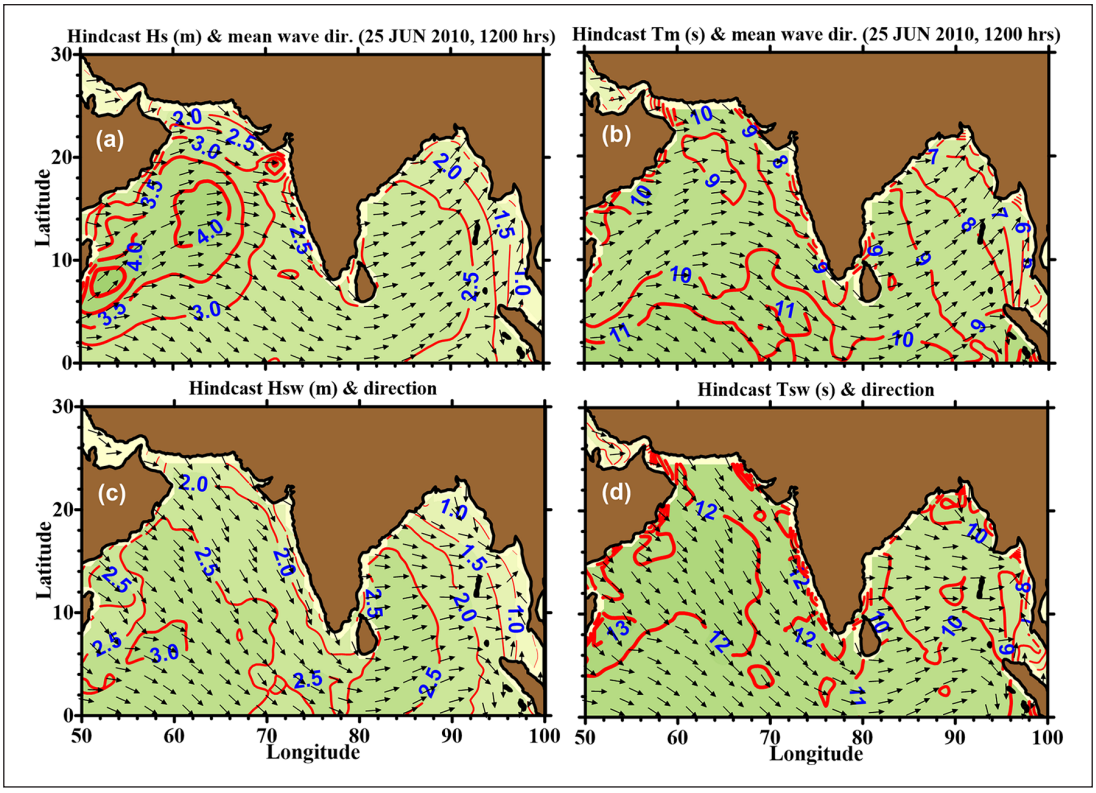

Figure 4. WAM hindcast wave fields (Hs, Tm, Hsw, and Tsw) using OSCAT winds, 25 June 2010, 12:00 hours.

Similarly, the WWIII hindcast wave fields such as Hs, Tm, Hsw, and Tsw and the wave directions for 25 January 2010, 12:00 hours, are shown in Figure 5. Hs varied from about 1.0 to 1.8 m in the Arabian Sea and from 0.8 to 1.4 m in the Bay of Bengal. Tm varied between 6 and 7 s in the Arabian Sea, whereas it varied from 6 to 8 s in the Bay of Bengal. The mean wave directions mostly agree with the input wind pattern. Hsw ranged from 1.2 to 1.6 m in the Arabian Sea and from 0.8 to 1.2 m in the Bay of Bengal. Tsw varied from 8 to 9 s in the Arabian Sea and from 6 to 8 s in the Bay of Bengal. Figure 6 shows the WWIII hindcast wave fields for 25 June 2010, 12:00 hours, using OSCAT winds. Here, Hs ranged between 2.0 and 4.0 m in the Arabian Sea and between 1.0 and 2.5 m in the Bay of Bengal. Tm varied from 6 to 9 s in the Arabian Sea and from 5 to 9 s in the Bay of Bengal. In the Bay of Bengal, Hsw varied from 1.5 to 3.0 m, whereas in the Arabian Sea, it varied from 1.0 to 2.5 m. Tsw varied in the Arabian Sea between 9 and 11 s, and in the Bay of Bengal, it varied between 6 and 9 s. In general, Figure 6 reveals the anticipated southwest monsoon wind and wave activity in the North Indian Ocean.

The OSCAT winds were also used as input to force the WAM/WWIII models for the preselected months of January and June 2011. The spatial distribution of sample input wind fields for the North Indian Ocean are shown for 25 January, 12:00 hours and 25 June, 12:00 hours of 2011 in Figure 7, which shows that the wind speed varied from 2 to 8 m/s and from 4 to 10 m/s, respectively, for 25 January 2011, 12:00 hours, and 25 June 2011, 12:00 hours. It may also be seen from these plots that the wind speed and direction for January and June 2011 again represent the standard climatic pattern of wind variability (Hastenrath and Lamb, 1979; Young and Holland, 1996), north-easterly for 25 January 2011, 12:00 hours and south-westerly for 25 June 2011, 12:00 hours. One important point to be noted here is that, the average wind in the Bay of Bengal (8–10 m/s) on 25 June 2011 was higher than that in the Arabian Sea (5–9 m/s). Such a scenario is usually encountered at the time of onset of southwest monsoon during which the southern Bay of Bengal experiences stronger winds compared to the eastern Arabian Sea (Swain, 1997). This is because the southwest monsoon sets over Andaman and Nicobar Islands before it reaches the west coast of India. However, in this case, the winds were equally strong (10 m/s covering a larger area) in the northern Bay compared with the southern Bay, which can be due to the presence of a system (depression/cyclone) in the Bay. On inspection of the monsoon 2011 report by the Indian Meteorological Department (IMD; Ajit and Pai, 2012), it is found that there was a depression over the Bay of Bengal during 16–23 June 2011, which is likely to be the causative factor for relatively higher wind and wave activity in this region on 25 June 2011 (12:00 hours) as shown in Figures 7(b) and 9.

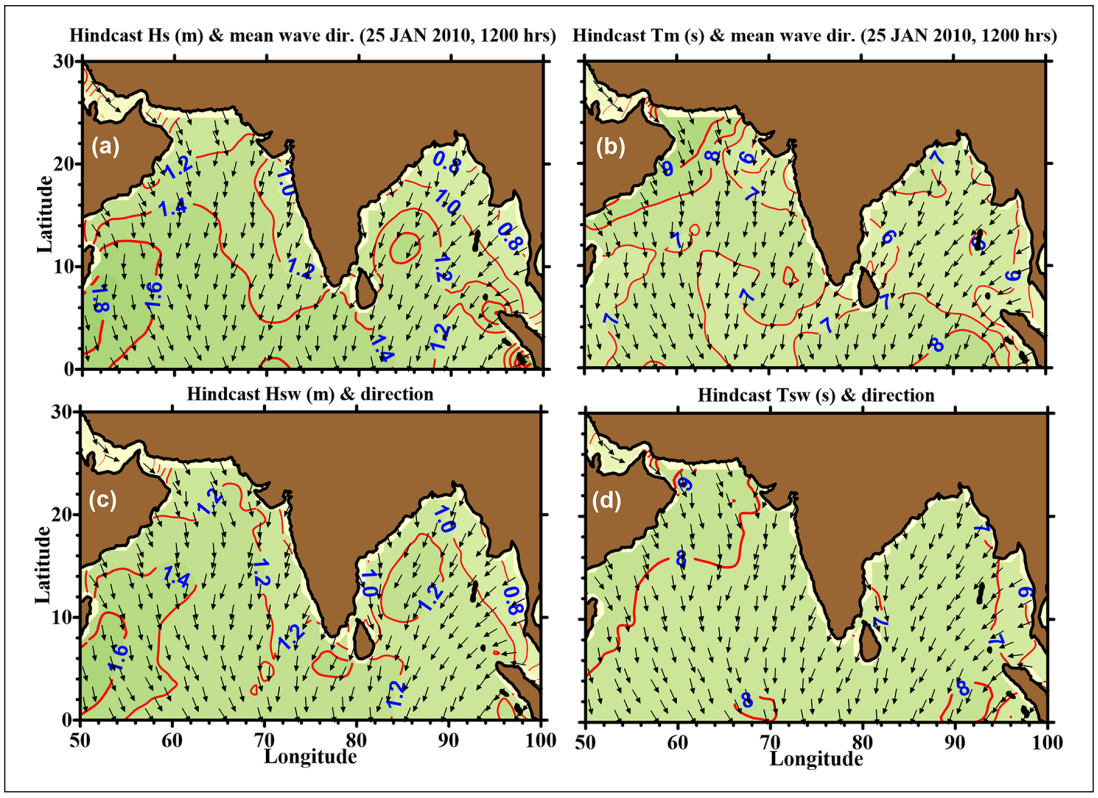

Figure 5. WWIII hindcast wave fields (Hs, Tm, Hsw, and Tsw) using OSCAT winds, 25 January 2010, 12:00 hours.

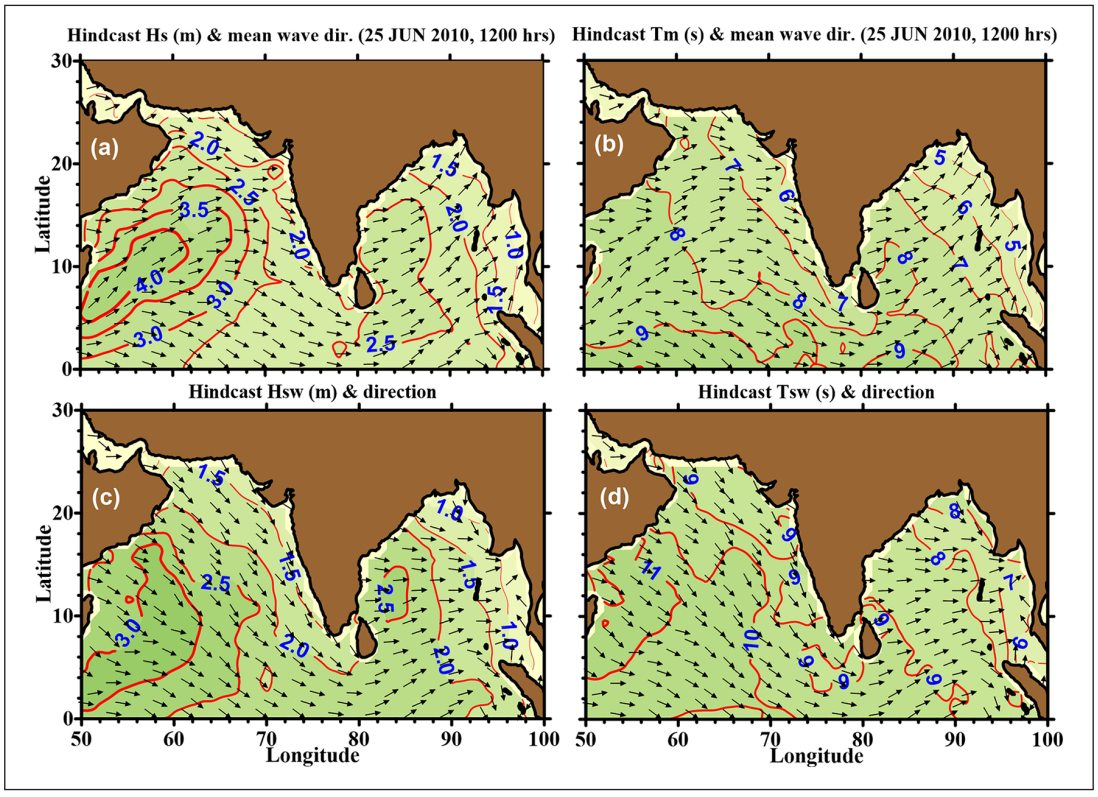

Figure 6. WWIII hindcast wave fields (Hs, Tm, Hsw, and Tsw) using OSCAT winds, 25 June 2010, 12:00 hours.

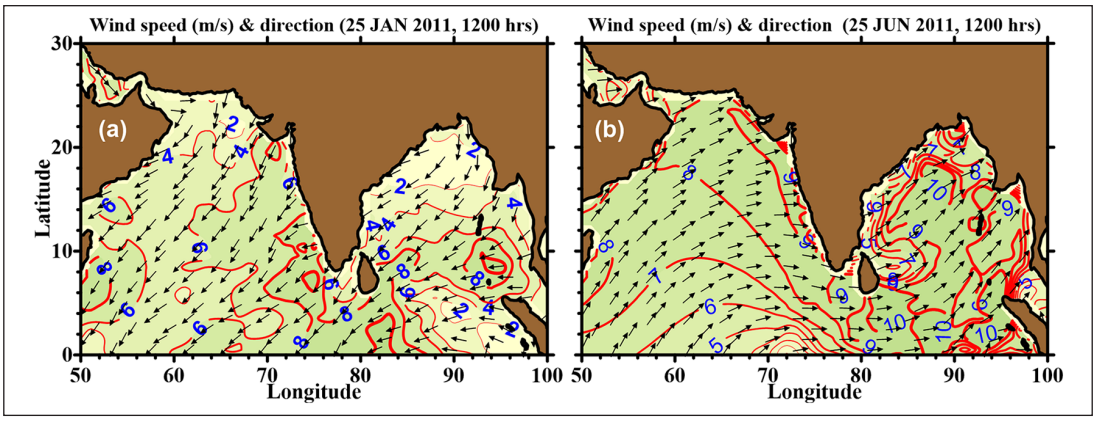

Figure 7. Input wind field (OSCAT), wind speed (m/s), and direction (arrows) for wave hindcast using WAM and WWIII for the North Indian Ocean, January and June 2011.

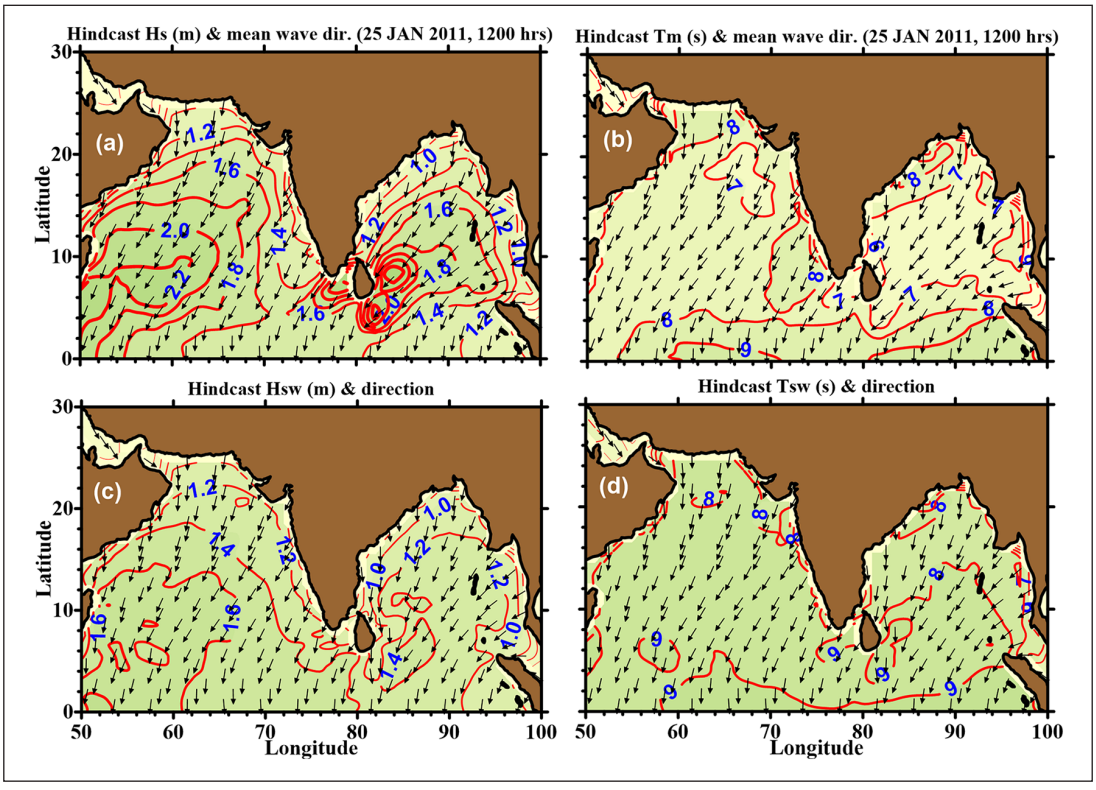

Figure 8. WAM hindcast wave fields (Hs, Tm, Hsw, and Tsw) using OSCAT winds, 25 January 2011, 12:00 hours.

The hindcast wave fields (WAM) for 25 January 2011, 12:00 hours, as shown in Figure 8, reveal that Hs varied from about 1.2 to 2.2 m in the Arabian Sea and from 1.0 to 2.4 m in the Bay of Bengal. Tm varied between 7 and 9 s in the Arabian Sea, whereas it varied from 6 to 9 s in the Bay of Bengal. The mean wave directions more or less agree with the prevailed wind pattern. Hsw ranged from 1.2 to 1.6 m in the Arabian Sea and from 1.0 to 1.4 m in the Bay of Bengal. Tsw varied from 8 to 9 s in the Arabian Sea and from 7 to 9 s in the Bay of Bengal. Figure 9 shows the WAM hindcast field for 25 June 2011, 12:00 hours, using OSCAT winds. The wind and wave conditions during the southwest monsoon period over the Indian Ocean remain generally high. Here, on 25 June 2011, Hs are in the range of 2–3 m in the Arabian Sea and 1.5–2.5 m in the Bay of Bengal. Tm varies from 7 to 11 s in the Arabian Sea and from 6 to 8 s in the Bay of Bengal. In the Bay of Bengal, Hsw varied from 1.0 to 2.0 m, whereas it ranged from 1.5 to 3.0 m in the Arabian Sea. Tsw is higher in the Arabian Sea (10–11 s) compared to that in the Bay of

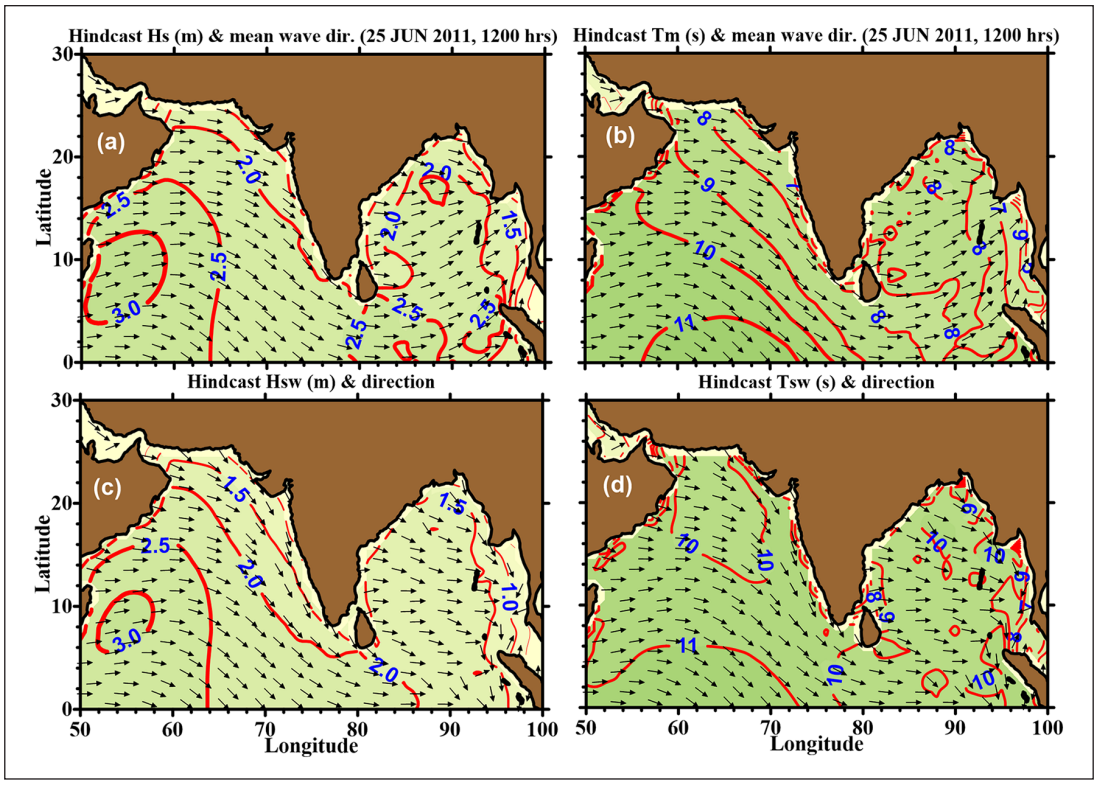

Figure 9. WAM hindcast wave fields (Hs, Tm, Hsw, and Tsw) using OSCAT winds, 25 June 2011, 12:00 hours.

Bengal (8–10 s). Hence, the predicted wave parameters Hs, Tm, Hsw, and Tsw and mean wave directions generally appeared to agree with the spatial distribution pattern of input wind field.

Similarly, in this case also, OSCAT winds are used as input to force the WWIII model for the preselected months of January and June 2011. The hindcast wave fields (25 January, 12:00 hours and 25 June, 12:00 hours of 2011) are shown in Figures 10 and 11, respectively, for January and June 2011. It may be seen from these plots that the wind and hindcast wave fields for January and June 2011 represent the standard climatic pattern of wind variability (Hastenrath and Lamb, 1979; Young and Holland, 1996). The detailed analysis on these hindcast results are discussed below for one of the selected output time steps (Hs, Tm, Hsw, and Tsw fields) for a typical day (25 January and 25 June 2011).

The hindcast wave fields (WWIII) for 25 January 2011, 12:00 hours, as shown in Figure 10, reveal that Hs varied from 1.0 to 2.2 m in the Arabian Sea and from 1.0 to 2.0 m in the Bay of Bengal. Tm varied between 6 and 7 s in the Arabian Sea, whereas it varied between 5 and 7 s in the Bay of Bengal. The mean wave directions more or less agree with the prevailed wind pattern. Hsw ranged from 1.2 to 1.8 m in the Arabian Sea and from 1.0 to 1.4 m in the Bay of Bengal. Tsw varied from 7 to 8 s both in the Arabian Sea and in the Bay of Bengal. This clearly revealed that the normal winter monsoon activity is equally strong both in the Arabian Sea and the Bay of Bengal. The sea-state was composed of both wind-seas and swell energy components as seen in Figure 10. Figure 11 shows the WWIII hindcast field for 25 June 2011, 12:00 hours, using OSCAT winds. Here, on 25 June 2011 (12:00 hours), the hindcast Hs was in the range of 1.5–3.0 m in the Arabian Sea and 1.5–2.5 m in the Bay of Bengal. Hindcast Tm varies from 6 to 9 s in the Arabian Sea and from 5 to 7 s in the Bay of Bengal. In the Bay of Bengal, Hsw varied from 1.0 to 2.0 m, whereas it ranged from 1.0 to 3.0 m in the Arabian Sea. Tsw is also higher in the Arabian Sea (8–10 s) compared to that in the Bay of Bengal (5–7 s). It may be noted that, the WWIII hindcast wave parameters Hs, Tm, Hsw, and Tsw and mean wave directions are generally in agreement with the prevailed input wind fields.

Validation of wave hindcasts

Validation of a model with measurements is an important step involved for improved wave prediction and analysis for the region of interest; hence, first, the model outputs were validated before attempting the intercomparison of WAM and WWIII. Based on the availability of buoy data pertaining to the study period and the region of interest, comparisons were made between the buoy- and model-derived wave heights and wave periods for January and

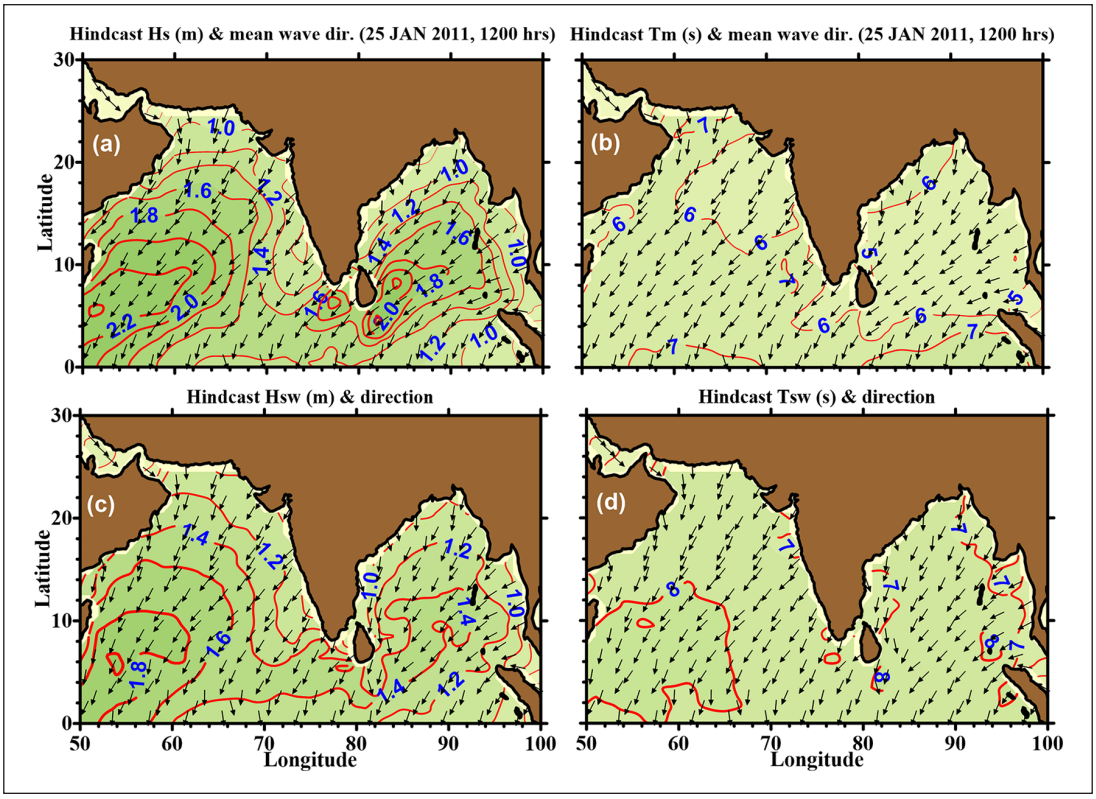

Figure 10. WWIII hindcast wave fields (Hs, Tm, Hsw, and Tsw) using OSCAT winds, 25 January 2011, 12:00 hours.

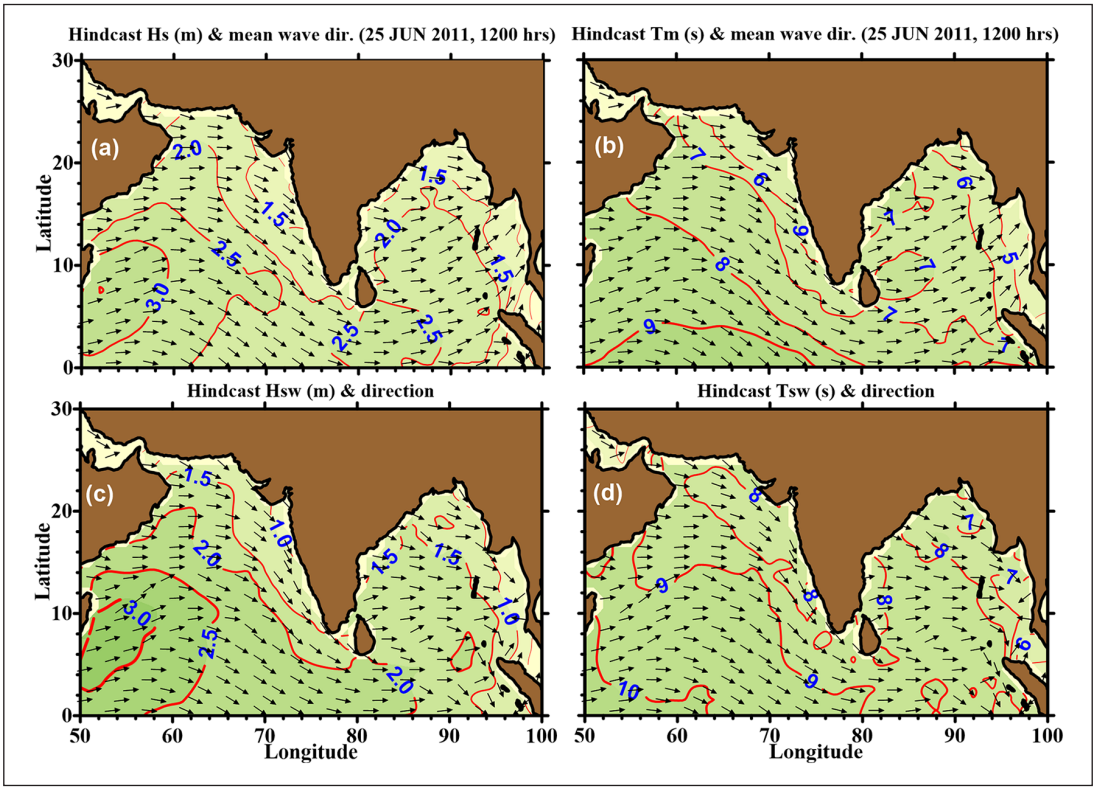

Figure 11. WWIII hindcast wave fields (Hs, Tm, Hsw, and Tsw) using OSCAT winds, 25 June 2011, 12:00 hours.

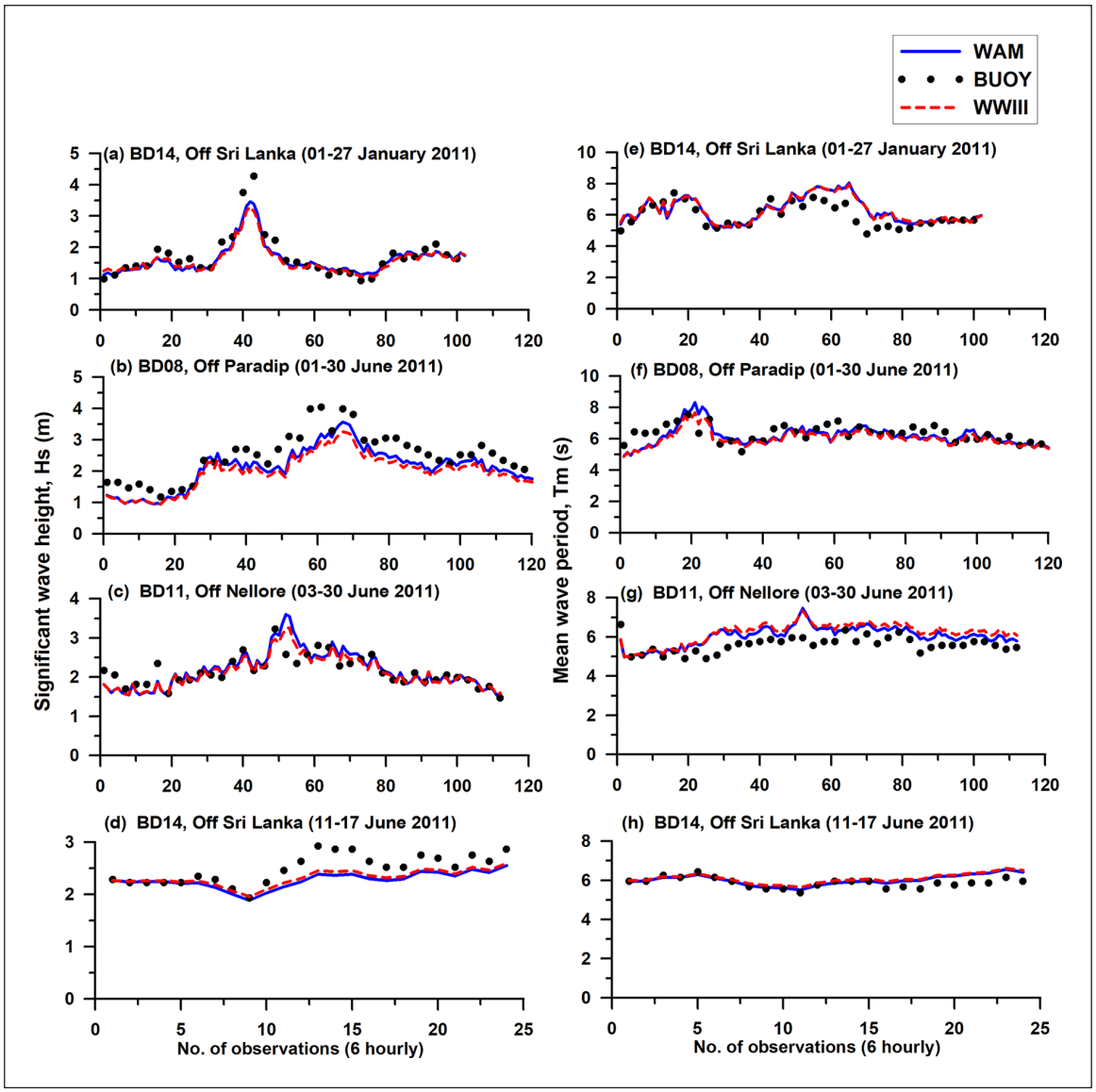

Figure 12. Comparisons between the observed (buoys), WAM, and WWIII predicted wave parameters at 6-hourly intervals for January and June 2011, using OSCAT winds.

June 2011. The in-situ met-ocean buoy parameters such as Hs and Tm of National Institute of Ocean Technology (NIOT; disseminated by INCOIS, Hyderabad) for the buoys located in the Bay of Bengal (shown in Figure 1) named BD08 (off Paradip; 18.19°N and 89.68°E), BD11 (off Nellore; 14.20°N and 82.92°E), and BD14 (off Sri Lanka; 6.19°N and 85.87°E) have been co-located with WAM and WWIII model outputs and interpolated in space and time for comparisons/validations. Table 1 shows the details of the hindcast studies and Figure 1 shows the locations of measured wave data used for the validation purpose. A statistical error analysis is performed for each dataset to evaluate the model performance. Figure 12 shows the comparisons between the observed and predicted wave parameters (Hs and Tm) at 6-hourly intervals for the period 1–27 January 2011 (BD14), 1–30 June 2011 (BD08), 3–30 June 2011 (BD11), and 11–17 June 2011 (BD14), respectively. In Figure 12, the WAM (continuous line in blue) and WWIII model outputs (dotted lines in red) are compared with measurements from three buoy (solid dots in black color) locations. The length of the time series or the number of data points plotted for comparison between the model and the buoy observations may vary due to missing buoy data.

Figure 12(a) shows considerable correlations between buoy BD14 (off Sri Lanka) and WAM hindcast parameters such as Hs and Tm using OSCAT data for the period 1–27 January 2011. The statistics of the comparison of WAM and WWIII model wave parameters with buoy measurements in the Bay of Bengal are shown in Table 2. The

Table 2. Statistics of the comparison of WAM and WWIII model wave parameters with buoy measurements in the Bay of Bengal as shown in Figure 12.

Statistical estimates	BD14 (January 2011)	BD08 (June 2011)	BD11 (June 2011)	BD14 (June 2011)
Significant wave height, Hs (m): WAM/WWIII				
R	0.98/0.98	0.96/0.97	0.86/0.89	0.85/0.94
SI	0.05/0.06	0.07/0.12	0.03/0.02	0.03/0.02
B	0.13/0.16	0.37/0.50	−0.01/0.05	0.22/0.17
RMSE	0.08/0.11	0.19/0.31	0.06/0.04	0.07/0.05
PE	9.8/11.1	19.0/25.7	7.5/7.0	9.5/7.6
MPI	0.95/0.94	0.92/0.88	0.97/0.98	0.97/0.98
Mean wave period, Tm (s): WAM/WWIII				
R	0.82/0.82	0.72/0.77	0.70/0.73	0.66/0.64
SI	0.07/0.06	0.04/0.04	0.05/0.08	0.01/0.02
B	−0.38/−0.38	0.17/0.33	−0.40/−0.57	−0.15/−0.22
RMSE	0.40/0.39	0.23/0.26	0.29/0.44	0.07/0.09
PE	7.3/7.4	6.0/6.8	7.2/9.3	3.0/3.8
MPI	0.93/0.94	0.96/0.96	0.95/0.92	0.99/0.98

R: correlation coefficient; SI: scatter index; B: bias; RMSE: root-mean-square error; PE: percentage error; MPI: model performance index.

correlation coefficients are 0.98 and 0.82 for Hs and Tm, respectively, with a low value of SI (0.05 and 0.07), which indicate better fits for both Hs and Tm. The bias is lower and positive (0.13) for Hs for the observed wave height range of 0.9–4.7 m, which reveals that the model could in general predict Hs at the buoy location. However, during the peak high wave activity period (maximum Hs up to 4.7 m), the model (WAM) could not reproduce a similar sea-state. This type of mismatch usually happens during a stronger wind/weather system, where the input/analyzed wind field that is used to drive the wave model does not reflect the observed wind variability for that particular wind/weather system, as in this case. RMSE is 0.08, which also indicates a better fit between the model and the observations. The estimated PE is 9.8% with MPI at 0.95, which reveals that the model could reproduce the observed wave characteristics (Hs) fairly well for the BD14 buoy location in the Bay of Bengal (south), except during the peak high wave activity period. Tm (Figure 12(e)) also shows reasonably good correlation (R = 0.82) with SI 0.07 and RMSE 0.40, which indicates better fit between the WAM and observations. The bias is negative (–0.38) with PE at 7.3% and MPI at 0.93, which also reveal good agreement between the model and the buoy for Tm.

Similarly, Figure 12(a) and (e) shows considerable correlations (Table 2) between the buoy BD14 and WWIII hindcast parameters such as Hs and Tm using OSCAT data. The correlation coefficients are 0.98 and 0.82 for Hs and Tm, respectively, with low value of SI (0.06 for Hs and Tm), which indicate better fit for both Hs and Tm. The bias is lower and positive (0.16) for Hs for the observed wave height range of 0.9–4.7 m, which reveals that the model could in general predict Hs at the buoy location. However, during the peak high wave activity period (maximum Hs up to 4.7 m), which was due to the influence of a prevailing depression in the southern Bay, the model (WWIII) could not reproduce the observed sea-state. The RMSE is 0.11, which also indicates better fit between the model and the observations. The estimated PE is 11.1% with MPI at 0.94, which also reveals that the model could reproduce the observed wave height (Hs) fairly well for the BD14 buoy location in the south central Bay, except during the peak high wave activity period. Tm also shows reasonably good correlation (R = 0.82) with SI at 0.06 and RMSE 0.39, which indicates better fit between the model and the observations. The bias is negative (–0.38) with PE at 7.4% and MPI at 0.94, which reveals good agreement for Tm between the model and the buoy.

The WAM and WWIII model hindcasts were also validated with buoys BD08, BD11, and BD14 (all located in the Bay of Bengal) for the periods 1–30 June, 3–30 June, and 11–17 June 2011, respectively, as shown in Figure 12(b) to (d). The estimated R values are 0.96, 0.86, and 0.85 for BD08, BD11, and BD14, respectively, with SI values of 0.07, 0.03, and 0.03 and RMSE at 0.19, 0.06, and 0.07, with all the estimates indicating better fit between the WAM model and the buoys for Hs during the prevailing active southwest monsoon winds. The bias is positive for BD08 (B = 0.37) and BD14 (B = 0.22), whereas it is negative for BD11 (−0.01), which is a negligibly small value. The values of PE are 19.0%, 7.5%, and 9.5% for BD08, BD11, and BD14, respectively, which indicate fairly good agreement for BD11 and BD14 compared with BD08. MPI is at 0.92 for BD08, and 0.97 for both BD11 and BD14. Tm (Figure 12(f) to (h)) shows relatively lower correlation such as 0.72 for BD08, 0.70 for BD11, and 0.66 for BD14 compared with Hs, as discussed above. SI is 0.04, 0.05, and 0.01 for BD08, BD11, and BD14, respectively, with

RMSE at 0.23, 0.29, and 0.07, which indicate a generally better fit between the model and buoys for Tm. Moreover, the computed values of bias such as 0.17 (BD08), −0.40 (BD11) and −0.15 (BD14) reveal that the WAM model could hindcast Tm well within an error of 0.5 second. The PE values are low at all the buoy locations such as BD08 (6.0%), BD11 (7.2%), and BD14 (3.0%). Values of MPI are 0.96 for BD08, 0.95 for BD11, and 0.99 for BD14, which also indicate good agreement between the WAM and buoy measurements.

Similarly, WWIII model hindcasts (Table 2) are also validated with buoys BD08, BD11, and BD14 for the period 1–30 June, 3–30 June, and 11–17 June 2011, respectively, as shown in Figure 12. The coefficients of correlation (R) between the hindcast and buoys (Figure 12(b) to (d)) are 0.97, 0.89, and 0.94 for BD08, BD11, and BD14, respectively, with SI values at 0.12, 0.02, and 0.02 and RMSE at 0.31, 0.04, and 0.05. All these estimates indicate a better fit between the model and buoys for Hs during the prevailing active southwest monsoon winds. The computed bias for Hs is positive, that is, 0.50, 0.05, and 0.17 for BD08, BD11, and BD14, respectively. The values of PE are 25.7%, 7.0%, and 7.6% for BD08, BD11, and BD14, respectively, which indicate a fairly good agreement for BD11 and BD14. In the case of BD08, the observed Hs is higher than the model hindcasts (PE = 25.7%). MPI is at 0.88 for BD08 and 0.98 for both BD11 and BD14. Tm (Figure 12(f) to (h)) shows relatively lower correlation such as 0.77 for BD08, 0.73 for BD11, and 0.64 for BD14 compared with Hs as discussed above. SI is 0.04, 0.08, and 0.02 for BD08, BD11, and BD14, respectively, with RMSE at 0.26, 0.44, and 0.09, which indicate a generally better fit between the model and buoy for Tm. Moreover, the computed values of bias are 0.33 (BD08), −0.57 (BD11), and −0.22 (BD14), which reveal that the WWIII model could simulate Tm well within an error of ±0.5 second. The PE values are low at all the buoy locations at BD08 (6.8%), BD11 (9.3%), and BD14 (3.8%). Values of MPI are 0.96 for BD08, 0.92 for BD11, and 0.98 for BD14, which further indicate good agreement between the WWIII and buoy measurements for Tm.

Overall, the comparisons were promising and both models performed fairly well in the model domains. It is to be noted that at the buoy locations, both WAM and WWIII have underestimated Hs and overestimated Tm, but with slightly better performances exhibited by WAM. Many reasons can be attributed to the deviations in Hs and Tm, such as the quality of input wind fields, model grid resolution, wave model numerics, and the physics driving the different representation of swell propagations in both the models. The performance of the WAM and WWIII models could be ascertained based on the above validation case studies discussed using in-situ measurements. Furthermore, intercomparison of the two models considered in this investigation will be presented in the subsequent sections.

Intercomparison of WAM and WWIII hindcasts

In this study, intercomparisons have been carried out for WAM and WWIII wave models using 6-hourly interpolated OSCAT winds for the four selected months of January and June 2010 and January and June 2011. The results reveal that, both WAM and WWIII hindcasts have a general agreement with each other. However, in this study their quantitative intercomparisons will be presented. As indicated earlier, a detailed statistical error analysis is also performed for the intercomparison of WAM and WWIII using OSCAT winds to evaluate relative model performances. WAM hindcasts are compared with WWIII with special emphasis on the North Indian Ocean region.

Intercomparison (WAM and WWIII) for January 2010. The scatterplots of the intercomparison of WAM and WWIII model hindcast parameters such as Hs, Tm, and Hsw for the month of January 2010 in the North Indian Ocean is as shown in Figure 13. Table 3 shows the statistical estimates of the intercomparison between the WAM and WWIII output parameters during January 2010. The hindcast wave parameters Hs, Tm, and Hsw show higher correlations of 0.94 (R), 0.97, and 0.94, respectively. The comparison for Hs predicted by both the models for the North Indian Ocean reveals SI of 0.02, bias of 0.03, RMSE of 0.03, and PE of 8.8. Similarly, the comparison for Tm shows bias of −0.11, SI of 0.02, RMSE of 0.15, and PE of 4.0; which reveal very good agreement between both the models. Hsw varied from 0.1 to 2.8 m in the North Indian Ocean during January 2010 with SI of 0.02 and bias of 0.07. RMSE for Hsw is 0.02 and PE is 9.8. The MPI values are 0.97 for Hs, and 0.98 for Tm as well as Hsw, which indicate very good agreement between WAM and WWIII. The values of PE suggest encouraging agreement between WAM and WWIII for all the three parameters considered, Hs (8.8), Hsw (9.8), and Tm (4.0).

Figure 14(a) to (d) shows the time series of the WAM and WWIII model wave parameters such as Hs and Tm for the selected locations E1 (12.15°N and 90.75°E), E2 (18.48°N and 87.55°E), E3 (8.69°N and 78.34°E), and E4 (13.10°N and 80.33°E) in the Bay of Bengal. It may be seen that, for the locations considered in the Bay of Bengal, the intercomparisons between WAM and WWIII for Hs show correlation coefficients of 0.74, 0.89, 0.91, and 0.87 at E1, E2, E3, and E4, respectively. The estimated values of bias are 0.05, 0.19, 0.34, and −0.03 for the selected locations E1, E2, E3, and E4, respectively. The PE values are between 7.2 and 23.7 for the locations considered and higher PE (23.7) is noticed only in the case of location E3.

The intercomparison for Tm (Figure 14(e) to (h)) also shows a higher correlation for the above-mentioned locations in the Bay of Bengal, that is, 0.97 for E4, 0.94 at E1, 0.99 at E2, and 0.89 at E3. B is positive for locations E2 (0.30) and E3 (0.13) and negative for E1 (−0.15) and E4

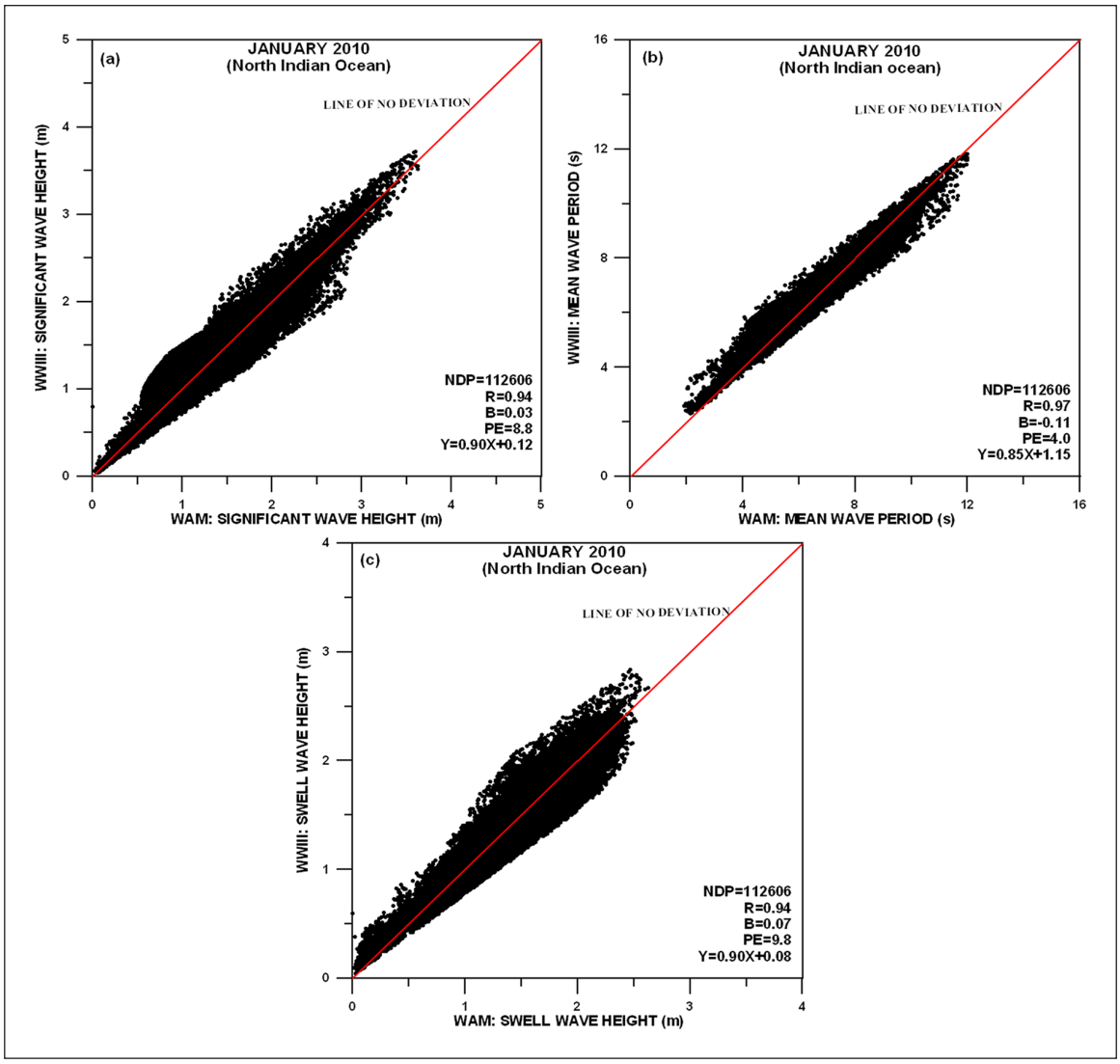

Figure 13. Intercomparison of WAM and WWIII model parameters for the North Indian Ocean (January 2010) using OSCAT winds.

Table 3. Statistical estimates (monthly) of the intercomparison between WAM and WWIII output parameters during January and June 2010 using OSCAT winds, as shown in Figures 13 and 15.

Statistical estimates	Significant wave height, Hs (m)		Mean wave period, Tm (s)		Swell wave height, Hsw (m)	
	January 2010	June 2010	January 2010	June 2010	January 2010	June 2010
Mean (WAM)	1.6	2.4	6.8	7.4	1.5	2.0
Range (WAM)	0.1–3.6	0.1–6.8	2.0–12.0	1.9–13.1	0.1–2.6	0.1–4.6
Mean (WWIII)	1.5	2.3	7.0	7.5	1.4	2.0
Range (WWIII)	0.1–3.7	0.1–5.9	2.3–11.8	2.2–11.7	0.1–2.8	0.1–4.4
R	0.94	0.96	0.97	0.99	0.94	0.96
SI	0.02	0.03	0.02	0.01	0.02	0.02
B	0.03	0.13	−0.11	0.04	0.07	0.04
RMSE	0.03	0.08	0.15	0.11	0.02	0.05
PE	8.8	10.8	4.0	3.4	9.8	9.6
MPI	0.97	0.97	0.98	0.98	0.98	0.98

R: correlation coefficient; SI: scatter index; B: bias; RMSE: root-mean-square error; PE: percentage error; MPI: model performance index.

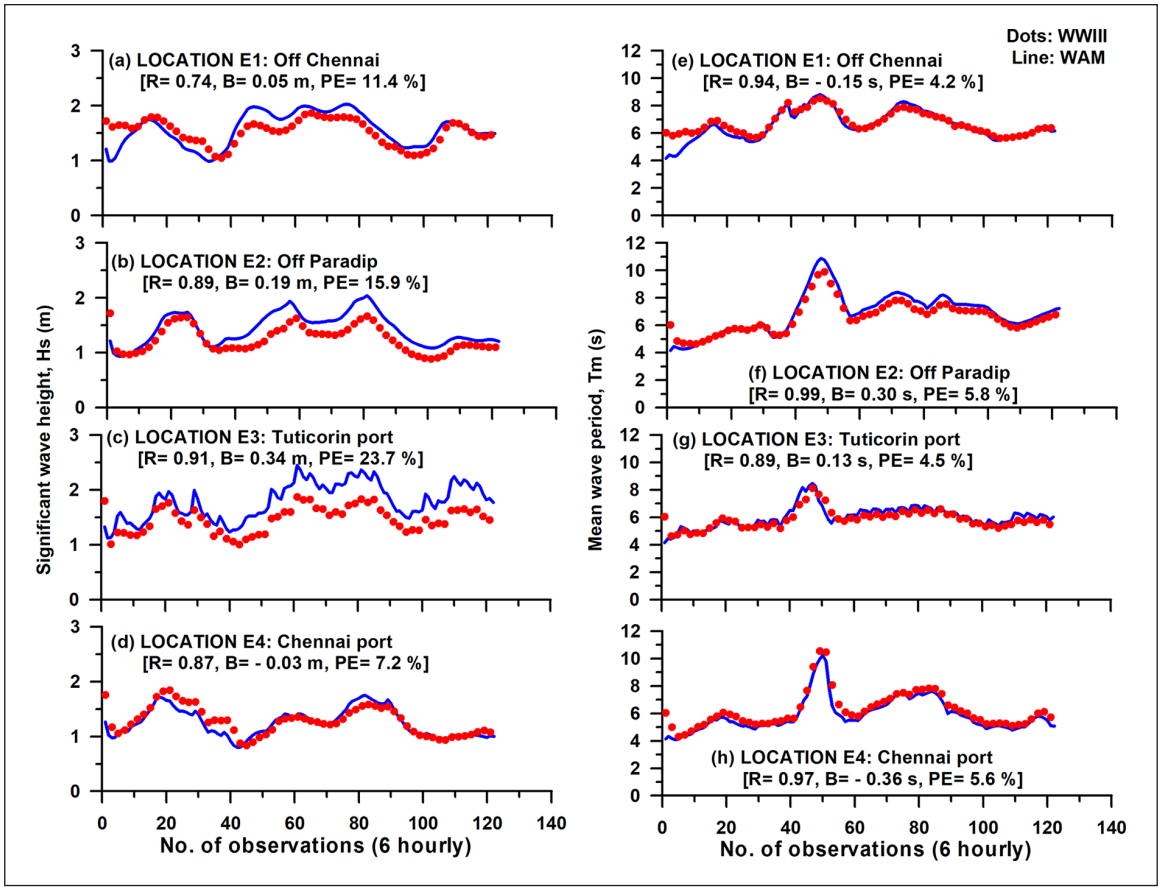

Figure 14. Time series of WAM and WWIII model wave parameters for selected locations in the Bay of Bengal for January 2010 using OSCAT winds.

(–0.36). The values of PE are less than 10 in all cases of Tm predicted by WAM and WWIII. Therefore, Figure 14 clearly reveals that the WAM and WWIII hindcasts for Hs deviate by 7%–24%, whereas Tm deviates by 4%–6%. Therefore, Tm shows better agreement between WAM and WWIII hindcasts compared to Hs, which deviates higher for one location (E3) as indicated above.

Intercomparison (WAM and WWIII) for June 2010. The intercomparison of WAM and WWIII model parameters (Hs, Tm, and Hsw) for the North Indian Ocean during June 2010 using OSCAT winds is shown in Figure 15. The hindcast wave parameters Hs, Tm, and Hsw show higher correlations of 0.96, 0.99, and 0.96, respectively, between WAM and WWIII. The intercomparison of Hs reveals SI of 0.03, bias of 0.13, RMSE of 0.08, and PE of 10.8. In the case of Tm, SI is 0.01, bias is 0.04, RMSE is 0.11, and PE is 3.4. Similarly, Hsw reveals SI of 0.02, bias of 0.04, RMSE of 0.05, and PE of 9.6. The value of MPI is 0.97 for Hs and 0.98 for both Tm and Hsw, which reveals strong agreement (Table 3) between the two models WAM and WWIII for the month of June 2010 in North Indian Ocean region.

Figure 16 shows the time series of WAM and WWIII model hindcast wave parameters Hs and Tm at the selected locations in the Arabian Sea (W1: 15.51°N and 69.25°E; W2: 10.57°N and 72.51°E; W3: 20.89°N and 71.49°E; and W4: 12.93°N and 74.72°E) and the Bay of Bengal (E1, E2, E3 and E4) during the month of June 2010. It may be noted that, for the locations in the Arabian Sea and the Bay of Bengal, the intercomparisons between WAM and WWIII for Hs show correlation coefficients ranging from 0.79 to 0.98 for the eight locations (Figure 16(a) to (h)). The values of B varied from −0.10 to 0.47, with PE in the range of 7%–23% for all the locations considered. The intercomparison for Tm (Figure 16(i) to (l)) also shows good correlation in the Arabian Sea, that is, 0.93, 0.96, 0.94, and 0.97 at W1, W2, W3, and W4 locations, respectively, while for buoy locations in the Bay of Bengal as shown in Figure 16(m) to (p), the correlation coefficients are 0.99 and 0.96 for locations E1 and E2, respectively, and 0.98 at E3 and E4, respectively. Bias is positive throughout (0.05–0.55) for all the locations expect at two locations, E3 (−0.06) and E4 (−0.18). Therefore, Figure 16 clearly reveals that WAM and WWIII hindcasts for Hs deviate from 7% to 23%, whereas Tm deviates from 1% to 9% (PE).

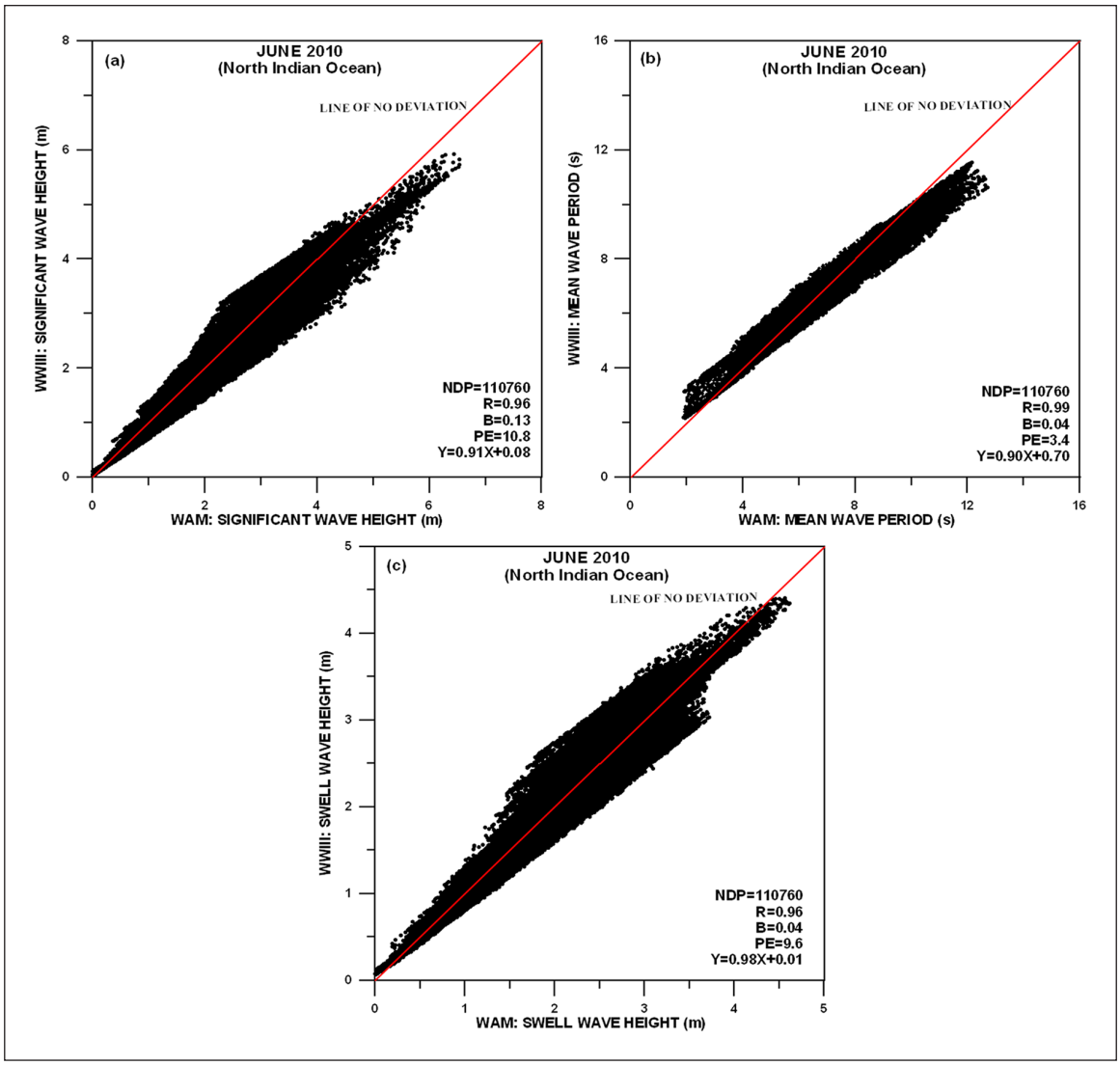

Figure 15. Intercomparison of WAM and WWIII model parameters for the North Indian Ocean (June 2010) using OSCAT winds.

Intercomparison (WAM and WWIII) for January 2011. The intercomparison of WAM and WWIII model hindcast parameters for the North Indian Ocean region during January 2011 using OSCAT winds is shown in Figure 17. The hindcast wave parameters Hs, Tm, and Hsw show strong correlations of 0.96, 0.98, and 0.94, respectively, between WAM and WWIII (Table 4). The comparison for Hs predicted by both the models in the North Indian Ocean region reveals SI of 0.02, bias of 0.07, RMSE of 0.01, and PE of 7.7. Similarly, the comparison for Tm shows bias of 0.04, SI of 0.02, RMSE of 0.05, and PE of 2.5, which reveal very good agreement between both the models. Hsw varied from 0.1 to 2.4 m in the North Indian Ocean during January 2011 with SI of 0.02 and bias of 0.06. The RMSE for Hsw is 0.02 and PE is 9.2. MPI is 0.99 for Hs, 0.98 for Tm, and 0.99 for Hsw, which indicate very good agreement between WAM and WWIII. The estimated PE at $<10\%$ revealed very good agreement between WAM and WWIII (Hs: 7.7, Hsw: 9.2, and Tm: 2.5).

Figure 18 shows the time series of WAM and WWIII model hindcast wave parameters Hs and Tm for the selected locations in the Bay of Bengal (E1, E2, E3, and E4) during the month of January 2011 using OSCAT winds. It may be seen that, for these locations, intercomparisons between WAM and WWIII for Hs (Figure 18(a) to (d)) show correlation coefficients of the order of 0.88–0.97. The values of bias varied from −0.01 to 0.20 with PE values of 6% and 18% among the locations considered in the Bay of Bengal.

The intercomparisons for Tm also show very good correlation in the Bay of Bengal (Figure 18(e) to (h)), with $R > 0.9$. B is positive at E1 (0.02) and E2 (0.24) but negative at E3 (−0.01) and E4 (−0.25). The values of PE are less

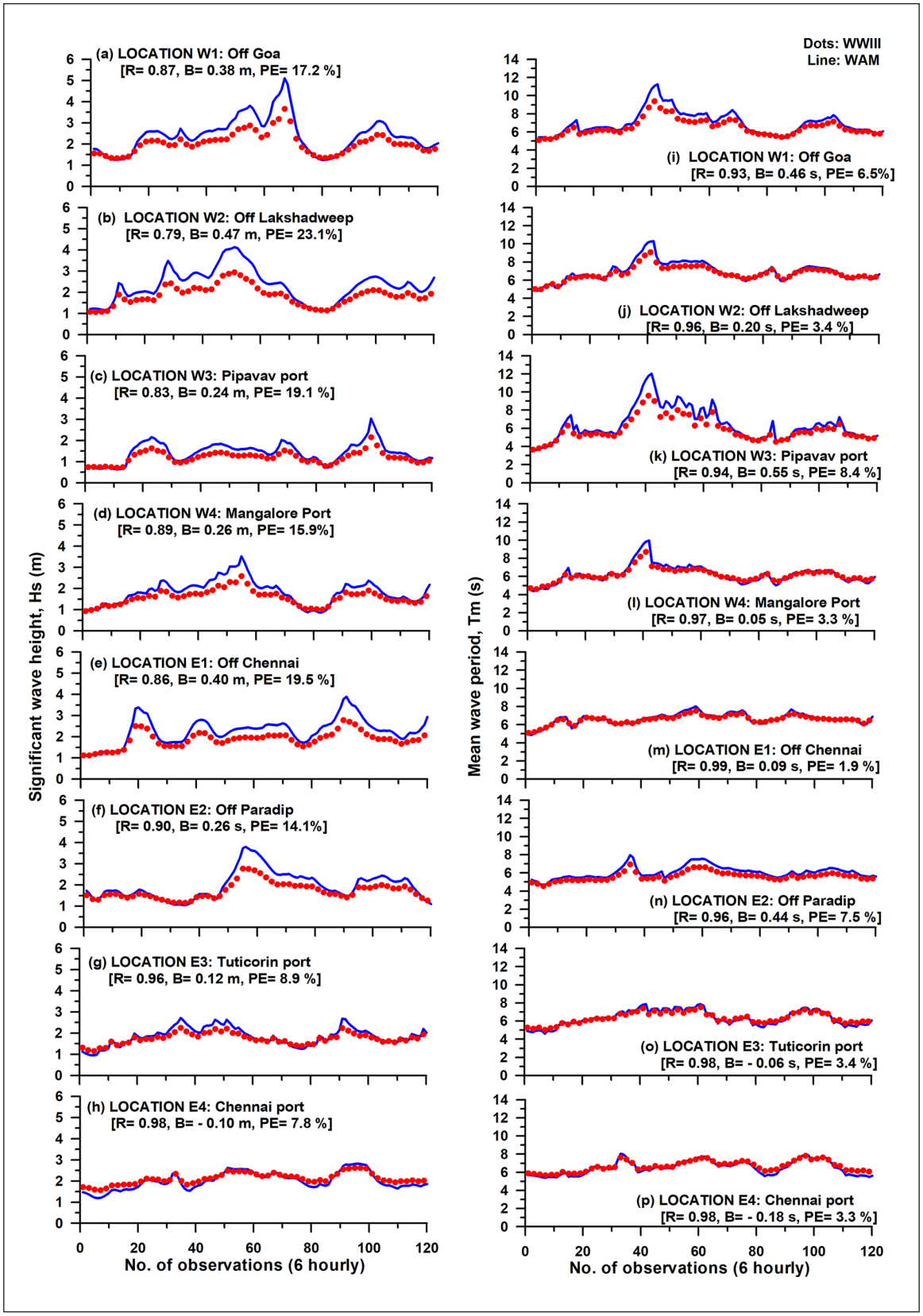

Figure 16. Time series of WAM and WWIII model wave parameters for selected locations in the Arabian Sea and the Bay of Bengal for June 2010 using OSCAT winds.

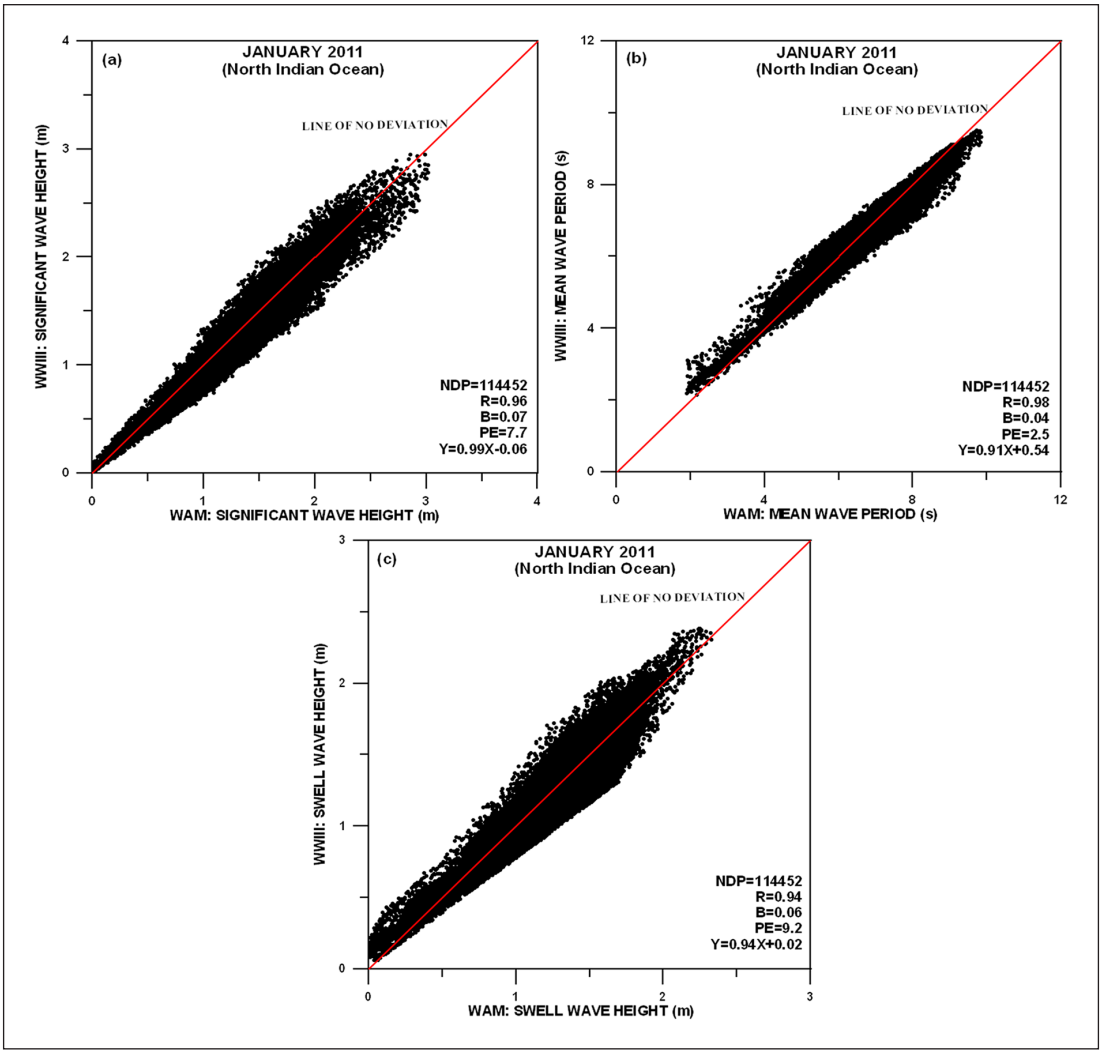

Figure 17. Intercomparison of WAM and WWIII model parameters for the North Indian Ocean (January 2011) using OSCAT winds.

Table 4. Statistical estimates of the intercomparison between WAM and WWIII output parameters during January and June 2011 using OSCAT winds as shown in Figures 17 and 19.

Statistical estimates	Significant wave height, Hs (m)		Mean wave period, Tm (s)		Swell wave height, Hsw (m)	
	January 2011	June 2011	January 2011	June 2011	January 2011	June 2011
Mean (WAM)	1.4	2.2	6.6	7.2	1.4	1.8
Range (WAM)	0.1–3.0	0.1–4.8	1.9–9.8	1.9–11.1	0.1–2.4	0.1–3.5
Mean (WWIII)	1.6	2.3	6.4	7.0	1.3	1.9
Range (WWIII)	0.1–2.8	0.1–4.2	2.1–9.5	2.0–10.4	0.1–2.4	0.1–3.4
R	0.96	0.98	0.98	0.97	0.94	0.98
SI	0.02	0.01	0.02	0.01	0.02	0.02
B	0.07	0.04	0.04	–0.02	0.06	0.01
RMSE	0.01	0.03	0.05	0.07	0.02	0.02
PE	7.7	6.1	2.5	3.0	9.2	3.5
MPI	0.99	0.99	0.98	0.99	0.99	0.99

R: correlation coefficient; SI: scatter index; B: bias; RMSE: root mean square error; PE: percentage error; MPI: model performance index.

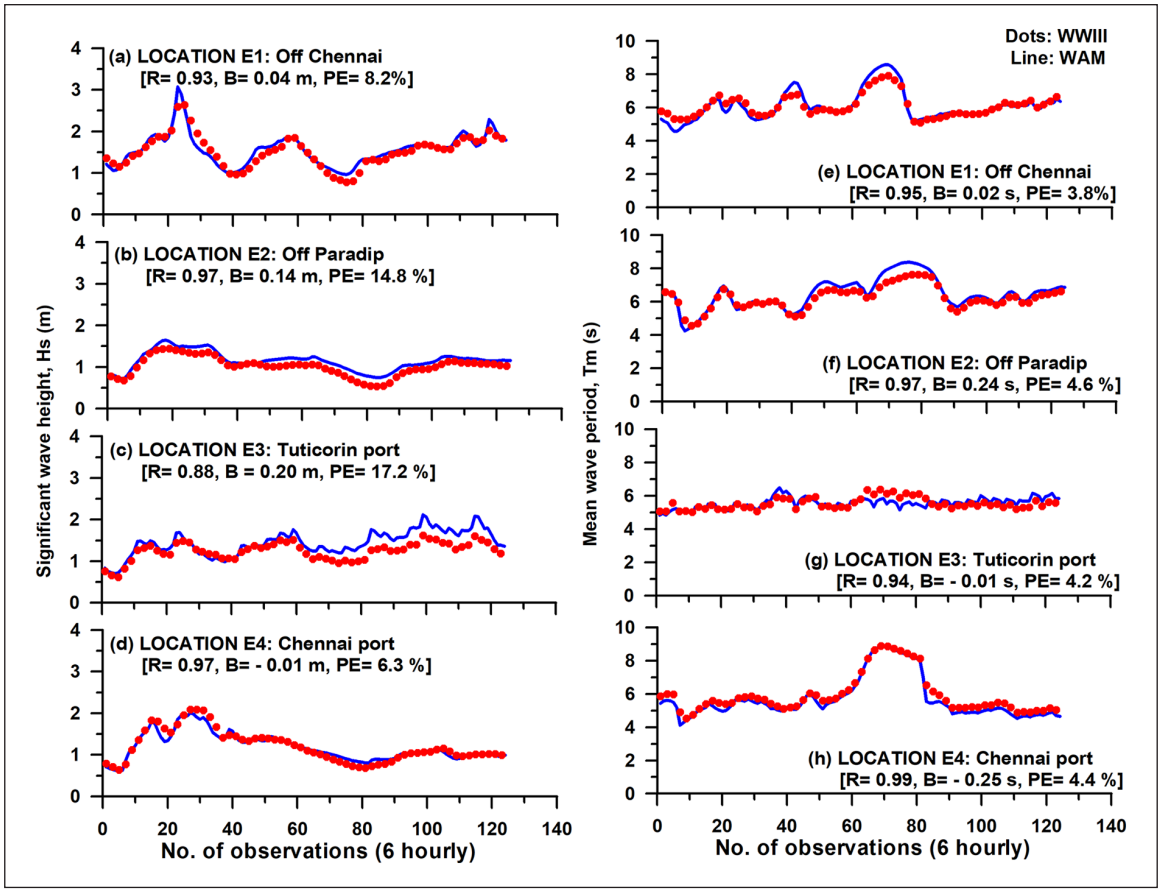

Figure 18. Time series of WAM and WWIII model wave parameters for selected locations in the Bay of Bengal for January 2011 using OSCAT winds.

than 5 considering all the cases for Tm predicted by WAM and WWIII. Therefore, Figure 18 clearly reveals that the WAM and WWIII hindcasts for Hs deviate from 6% to 18%, whereas Tm deviates from 3% to 5% only.

Intercomparison (WAM and WWIII) for June 2011. The scatterplots of the intercomparison of WAM and WWIII model parameters (Hs, Tm, and Hsw) for the North Indian Ocean region in the month of June 2011 using OSCAT winds is shown in Figure 19. The hindcast wave parameters Hs, Tm, and Hsw show higher correlations of 0.98, 0.97, and 0.98, respectively, between WAM and WWIII. The intercomparison of Hs reveals SI of 0.01, bias of 0.04, RMSE of 0.03, and PE of 6.1. In the case of Tm, SI is 0.01, bias is −0.02, RMSE is 0.07, and PE is 3.0. In the same way, Hsw reveals SI of 0.02, bias of 0.01, RMSE of 0.02, and PE of 3.5 (Table 4). The value of MPI is 0.99 for all the parameters Hs, Tm, and Hsw, which reveal strong agreement between the models WAM and WWIII for the month of June 2011 in the North Indian Ocean region. Here, it may be noted that the deviations between WAM and WWIII for all the three parameters are $<7\%$.

Figure 20 shows the time series of WAM and WWIII model wave parameters Hs and Tm for selected locations in the Bay of Bengal (E1, E2, E3, E4) during the month of June 2011 using OSCAT winds. It may be seen that, for the locations in the Bay of Bengal, the intercomparisons between WAM and WWIII for Hs (Figure 20(a) to (d)) show correlation coefficients varying from 0.89 to 0.98 for the locations considered, which is representative of a good comparison. The values of bias varied in the order of −0.08 to 0.24 with PE values ranging between 4% and 15% at all the locations considered. The intercomparison for Tm (Figure 20(e) to (h)) also shows good correlation ($R > 0.95$) for all the locations, with bias of the order of −0.30 to 0.31. The values of PE are less than 5% in all the locations for Tm predicted by WAM and WWIII. Therefore, Figure 20 clearly reveals that the WAM and WWIII hindcasts for Hs deviate from 4% to 15%, whereas Tm deviates from 2% to 5%. The month of June 2011 being that of the southwest monsoon, it is seen that in most cases the intercomparisons of Hs, Tm, and Hsw between WAM and WWIII reveal higher agreements compared to fair weather period.

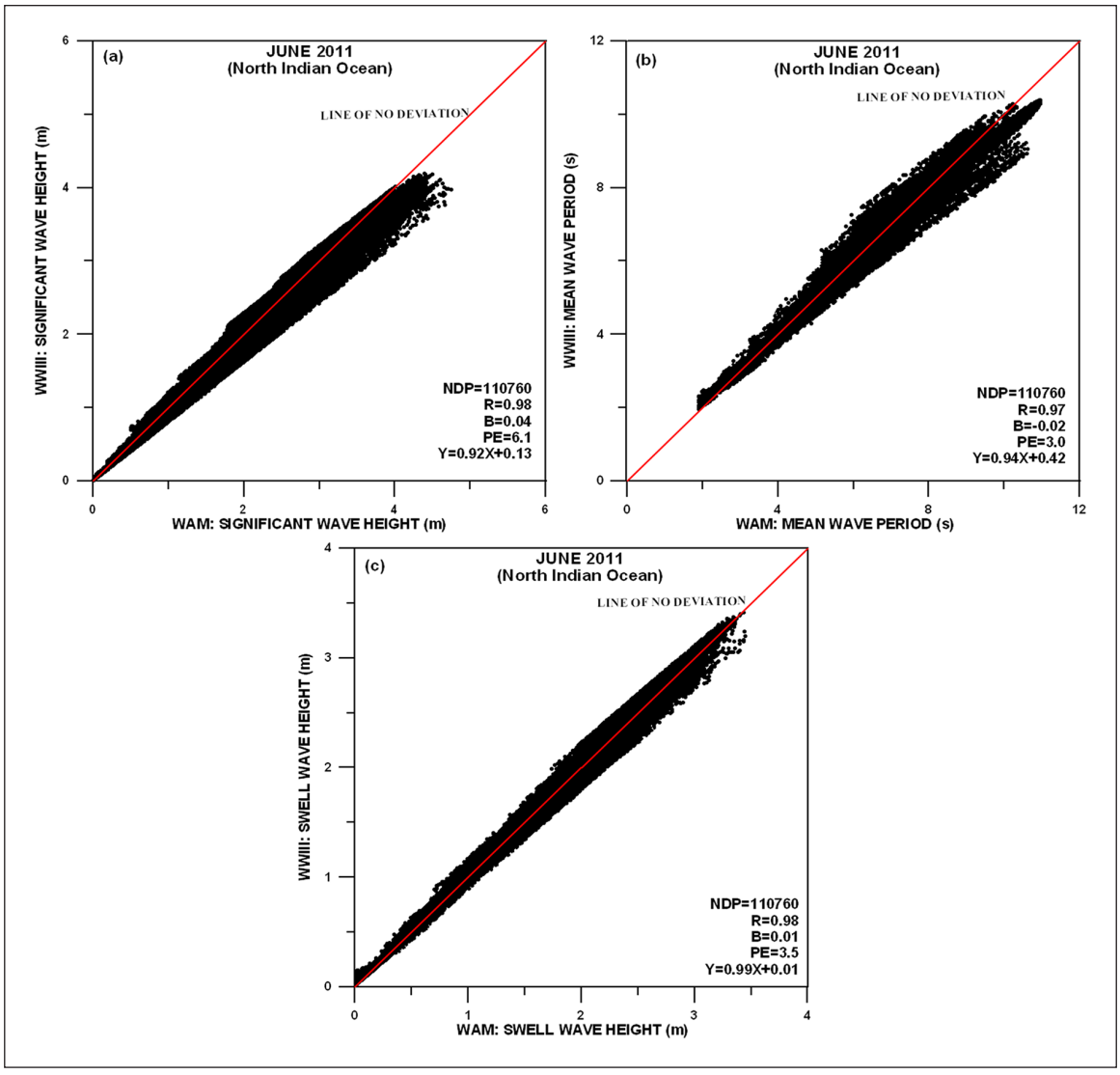

Figure 19. Intercomparison of WAM and WWIII model parameters for the North Indian Ocean (June 2011) using OSCAT winds.

Overall, taking into consideration the intercomparisons for the selected months and the time-series comparisons using WAM and WWIII at selected locations in the North Indian Ocean, it is noted that both the models performed reasonably well in the model domain considered, with slightly better performance demonstrated by WAM. PE varied in the range of 2.5%–10.8% for Hs, Tm, and Hsw in all the months considered, which is quite promising. However, from the monthly scatterplots, WAM hindcasts were relatively better than WWIII, considering all the case studies for the North Indian Ocean. Similarly, from the time-series comparisons at selected locations in the Arabian Sea and Bay of Bengal, it is noted that WAM performed better than WWIII with PE ranging from 1.9% to 23.7% for Hs and Tm. The deviations in the model performances can be primarily attributed to the quality of input winds, mainly the grid resolutions, numerics, and the physics driving these models. Whereas it may be noted that WWIII is the latest model that uses most recent physics of wave generation, wave–current interaction, and air–sea temperature difference as an additional input, and its numerical approaches are superior to WAM. WWIII offers several advantages over WAM as follows: WWIII adopts a third-order skillful wave propagation scheme that cuts down the numerical diffusion of swell energy distinctive of the first-order scheme applied in WAM. Also, WWIII has been set up to execute accurately on shared memory computers. The introduction of improved input-dissipation parameterization schemes in the latest versions of WWIII also adds to other advancements over WAM. Therefore, it would be wise to have long-term measurements both in deep and coastal waters of the North Indian Ocean to validate and intercompare WAM and WWIII further, coupled with SWAN in the nearshore waters.

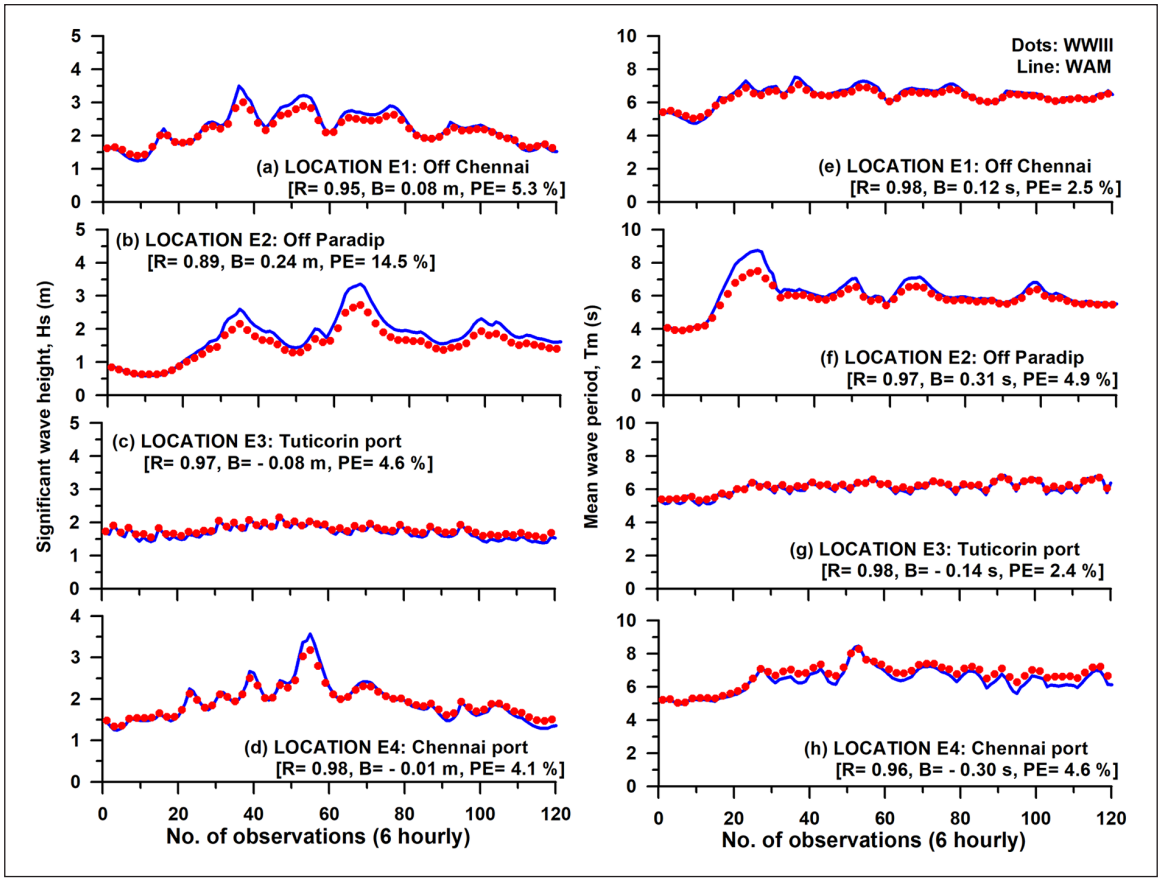

Figure 20. Time series of WAM and WWIII model wave parameters for selected locations in the Bay of Bengal for June 2011 using OSCAT winds.

Conclusion

The state-of-the-art third-generation wave models have been implemented (WAM Cycle 4.5.3 and WWIII: V3.14) in this study for their intercomparisons using OSCAT winds. This is the first and one of the initial attempts to study the intercomparison of wave hindcasts using third-generation wave models, such as WAM and WWIII, for the North Indian Ocean. Wave parameters obtained from the hindcasts are analyzed to understand the quality and variability associated with the individual model outputs. WAM and WWIII intercomparison studies have been carried out for four different cases such as January and June 2010, and January and June 2011 utilizing hindcast outputs (significant wave parameters) such as Hs, Tm, and Hsw through an extensive and robust statistical error analysis. The validations of the WAM and WWIII models using NIOT buoy measurements indicate that during the month of January and June 2011, the performance of WAM was slightly better than WWIII. The observed and predicted wave parameters of WAM and WWIII show PE ranging from 7% to 25% for Hs and within 10% for Tm. PE from the WWIII model compared to WAM was higher for Hs by 1%–6%. In addition, it is higher by 1%–3% in the case of Tm.

The case studies reveal that, the intercomparisons of WAM and WWIII in the North Indian Ocean are highly encouraging for January and June with percentage deviation for Hs, Tm, and Hsw ranging from 2% to 11%. The hindcast Tm of WAM and WWIII using OSCAT winds were in better agreement with each other (deviation $<5\%$) compared with Hs and Hsw. Intercomparison of wave hindcasts in the Arabian Sea remained generally better than that in the Bay of Bengal. Based on the quantitative and qualitative assessments of the model results, this study clearly indicates that the models WAM and WWIII performed well using OSCAT winds and they can be confidently used for long-term hindcasting for varied applications in the North Indian Ocean.

Acknowledgements

The authors express their sincere thanks to the Director, Group Head, Ocean Science Group of NPOL (Naval Physical and Oceanographic Laboratory) for their encouragement and facilities provided to carry out this work. This is part of the Ph.D. work of P. A. Umesh, carried out at NPOL, DRDO, Cochin, under a collaborative project between NPOL and Space Applications Centre (SAC), Ahmedabad (Project: NPOL/SAC-II). The authors express their sincere thanks to Director, SAC and Director, NRSC for

providing the required wind data used for execution of the wave model. They are also thankful to fellow scientists of the Data Management Division, Ocean Science Group, NPOL for their timely support and encouragement. Most importantly, all the organizations that have provided data for this study are gratefully acknowledged.

Declaration of conflicting interests

The author(s) declared no potential conflicts of interest with respect to the research, authorship, and/or publication of this article

Funding

The author(s) received no financial support for the research, authorship, and/or publication of this article.

ORCID iD

PA Umesh https://orcid.org/0000-0001-8217-7413

References

Ajit T and Pai DS (2012) *Monsoon 2011 report*. IMD Met Monograph: Synoptic Meteorology No. 01/2012. Pune, India: National Climate Centre, India Meteorological Department.

Amrutha MM, Sanil Kumar V, Sandhya KG, et al. (2016) Wave hindcast studies using SWAN nested in WAVEWATCH III—Comparison with measured nearshore buoy data off Karwar, eastern Arabian Sea. *Ocean Engineering* 119: 114–124.

Balakrishnan Nair TM, Remya PG, Harikumar R, et al. (2014) Wave forecasting and monitoring during very severe cyclone Phailin in the Bay of Bengal. *Current Science* 106: 1121–1125.

Balakrishnan Nair TM, Sirisha P, Sandhya KG, et al. (2013) Performance of the ocean state forecast system at Indian National Centre for Ocean Information Services. *Current Science* 105: 175–181.

Battjes JA (1994) Shallow water WAM. In: *Proceedings of international symposium: waves–physical and numerical modeling* (ed M Isaacson and M Quick), Vancouver, BC, Canada, 21–24 August, pp. 1–24. Vancouver, BC, Canada: Department of Civil Engineering, University of British Columbia.

Bidlot J, Janssen P and Abdalla S (2005) *A revised formulation for ocean wave dissipation in CY29R1*. File: R60.9/JB/0516. Reading: Memorandum Research Department of ECMWF.

Bonjean F and Lagerloef GSE (2002) Diagnostic model and analysis of the surface currents in the tropical Pacific Ocean. *Journal of Physical Oceanography* 32: 2938–2954.

Booij N, Holthuijsen LH and Ris RC (1999) A third-generation wave model for coastal regions. 1. Model description and validation. *Journal of Geophysical Research* 104: 7649–7666.

Brown JM (2010) A case study of combined wave and water levels under storm conditions using WAM and SWAN in a shallow water application. *Ocean Modelling* 35: 215–229.

Chakraborty A and Raj Kumar (2013) Generation and validation of analysed wind vectors over the global oceans. *Remote Sensing Letters* 4(2): 114–112.

Gunther H and Behrens A (2011) The WAM model-validation document version 4.5.3. Helmholtz-Zentrum Geesthacht (HZG), Centre for Materials and Coastal Research, Teltow.

Gunther H, Hasselmann S and Jansen PAEM (1992) *Wamodel, Cycle-4 (revised version)*. Technical report no. 4. Hamburg: Dautsches Klima Rechen Zentrum.

Hanson JL, Tracy BA, Tolman HL, et al. (2009) Pacific hindcast performance of three numerical wave models. *Journal of Atmospheric and Oceanic Technology* 26: 1614–1633.

Hastenrath S and Lamb PJ (1979) *Climatic Atlas of the Indian Ocean, Part-I: Surface Climate and Atmospheric Circulation*. Madison, WI: The University of Wisconsin Press.

Hersbach H and Janssen PAEM (1999) Improvements of the short fetch behavior in the WAM model. *Journal of Atmospheric and Oceanic Technology* 16: 884–892.

Holthuijsen LH (2007) *Waves in Oceanic and Coastal Waters*. Cambridge: Cambridge University Press.

Janssen PAEM (2008) Progress in ocean wave forecasting. *Journal of Computational Physics* 227: 3572–3594.

Jayaram C, Udaya Bhaskar TVS, Swain D, et al. (2014) Daily composite winds from Oceansat-2 scatterometer. *Remote Sensing Letters* 5: 258–267.

Komen GJ, Cavaleri L, Donelan M, et al. (1994) *Dynamics and Modelling of Ocean Waves*. Cambridge: Cambridge University Press.

Korres G, Papadopoulos A, Katsafados P, et al. (2011) A 2-year inter-comparison of the WAM-Cycle 4 and the WAVEWATCH-III wave models implemented within the Mediterranean Sea. *Mediterranean Marine Science* 12: 129–152.

Lavrenov IV (2003) A numerical study of a nonstationary solution of the Hasselmann equation. *Journal of Physical Oceanography* 33: 499–511.

Nayak S, Bhaskaran PK, Venkatesan R, et al. (2013) Modulation of local wind waves at Kalpakkam from remote forcing effects of Southern Ocean swells. *Ocean Engineering* 64: 23–35.

Ortiz-Royero JC and Mercado-Irizarry A (2008) An inter-comparison of SWAN and WAVEWATCH III models with data from NDBC-NOAA buoys at oceanic scales. *Coastal Engineering Journal* 50: 1–27.

Padilla-Hernandez R, Perrie W, Toulany B, et al. (2007) Modeling of two Northwest Atlantic storms with third-generation wave models. *Weather and Forecasting* 22: 1229–1242.

Polnikov VG, Dymov VI, Pasechnik TA, et al. (2007) Real merits of the wind wave model with an optimized source function. *Doklady Earth Sciences* 417: 1375–1379.

Remya PG, Kumar R, Basu S, et al. (2012) Wave hindcast experiments in the Indian Ocean using MIKE21 SW model. *Journal of Earth System Science* 121: 385–392.

Ris RC, Holthuijsen LH and Booij N (1999) A third-generation wave model for coastal regions: 2. Verification. *Journal of Geophysical Research, Oceans C* 4: 7667–7681.

Rusu E (2011) Strategies in using numerical wave models in ocean/coastal applications. *Journal of Marine Science and Technology* 19: 58–75.

Sabique L, Annapurnaiah K, Balakrishnan Nair TM, et al. (2012) Contribution of Southern Indian Ocean swells on the wave heights in the Northern Indian Ocean–A modeling study. *Ocean Engineering* 43: 113–120.

Sandhya KG, Balakrishnan Nair TM, Bhaskaran PK, et al. (2014) Wave forecasting system for operational use and its validation at coastal Puducherry, east coast of India. *Ocean Engineering* 80: 64–72.

Sudha AK and Prasada Rao CVK (2013) Comparison of Oceansat-2 scatterometer winds with buoy observations over the Indian Ocean and the Pacific Ocean. *Remote Sensing Letters* 4(2): 171–179.

Swain J (1997) *Simulation of wave climate for Indian Seas*. PhD Thesis, Cochin University of Science and Technology, Cochin, India.

Swain J, Umesh PA and Murty ASN (2017) Demonstration of an efficient interpolation technique of inverse time and distance for Oceansat-2 wind measurements at 6-hourly intervals. *International Journal of Ocean and Climate Systems* 8: 101–112.

SWAMP Group (1985) *Ocean Wave Modelling*. New York: Plenum Press.

SWAN Team (2011) *User Manual SWAN Cycle III Version 40.85*. Delft University of Technology, Delft. Available at: http://www.swan.tudelft.nl

Tolman HL (1991) A third-generation model for wind waves on slowly varying, unsteady and inhomogeneous depths and currents. *Journal of Physical Oceanography* 21: 782–797.

Tolman HL (2009) *User manual and system documentation of WAVEWATCH III TM Version 3.14*. NOAA/NWS/NCEP/MMAB Technical note 276. Available at: https://polar.ncep.noaa.gov/mmab/papers/tn276/MMAB_276.pdf

Tolman HL and Chalikov DV (1996) Source terms in a third-generation wind-wave model. *Journal of Physical Oceanography* 26: 2497–2518.

Tolman HL, Balasubramaniyan B, Burroughs LD, et al. (2002) Development and implementation of wind generated ocean surface wave models at NCEP. *Weather and Forecasting* 17: 311–333.

Udaya Bhaskar TVS, Jayaram C, Bansal S, et al. (2016) Generation and validation of two day composite wind fields from Oceansat-2 scatterometer. *Journal of Indian Society of Remote Sensing* 45: 113–122.

Vledder G (2001) Extension of the discrete interaction approximation for putting nonlinear quadruplet wave–wave interactions in operational wave models. In: *4th ASCE international symposium on ocean waves, measurement and analysis*, San Francisco, CA, 2–6 September, pp. 540–549. Reston, VA: ASCE.

WAMDI Group (1988) The WAM model—A third generation ocean wave prediction model. *Journal of Physical Oceanography* 18(12): 1775–1810.

Warner JC, Armstrong B, He R, et al. (2010) Development of a coupled ocean atmosphere–wave–sediment transport (COAWST) modeling system. *Ocean Modelling* 35: 230–244.

WISE Group (2007) Wave modelling—The state of the art. *Progress in Oceanography* 75: 603–674.

Young IR and Holland GJ (1996) *Atlas of the Oceans: Wind and Wave Climate*. New York: Pergamon, Elsevier Science Ltd.

Zeng X, Ruoying He, Zuo Xue, et al. (2015) River-derived sediment suspension and transport in the Bohai, Yellow, and East China Seas: A preliminary modeling study. *Continental Shelf Research* 111: 112–125.

Author biographies

J Swain received his M.Sc. (1982) and M.Phil. degree (1984) in Oceanography from Berhampur University (BU), Odisha, India; and Ph.D. in Marine Science (Physical Oceanography) from Cochin University of Science and Technology (CUSAT), Kochi, India, in 1998. He retired as a Scientist-"G" from Naval Physical and Oceanographic Laboratory, DRDO, Ministry of Defence, Kochi, India. His research interests include ocean wave modelling, ocean data management, prediction of uncertainty in coastal and nearshore ocean models, and wind-wave analysis/climate studies.

PA Umesh is currently a Post-Doctoral Fellow at Department of Civil Engineering, Indian Institute of Technology, Bombay. He received his master's degree in Physics from the School of Pure & Applied Physics, Mahatma Gandhi University, in 2004 and M.Tech. in Atmospheric Sciences from Cochin University of Science and Technology, Kerala, India, in 2006. He was awarded the Ph.D. degree (2015) in Marine Science (Oceanography) from Naval Physical and Oceanography Laboratory (under Cochin University of Science and Technology). His research interest includes ocean wave modelling, coastal engineering, coastal/nearshore wave transformation, and wind-wave climate studies by spectral modelling and development.

AN Balchand holds a master's degree in Oceanography (1980) from Cochin University of Science and Technology, India [CUSAT] followed by a doctoral degree (1984) in the field of Environmental Oceanography. As a post doctoral Commonwealth Scholarship (1985) holder at erstwhile IMER, (currently PML, UK) he acquired enhanced skills in Estuarine and Coastal Oceanography. Thence, devoting past 32 years in the field of marine sciences, and serving CUSAT since 1990, both as a teaching cum research faculty, he recently retired as the Dean and Professor from the Faculty of Marine Sciences. To his credit, publications number more than 100, as dozens of doctoral and post graduate theses / dissertations decorate his stance. Active in academics, currently he is pursing topics in climate change related to coastal oceanography while continuing with teaching assignments.